Quantum Error Correction

and

Z(2) Lattice Models

Seyong Kim
Department of Physics
Sejong University

Quantum Computing is "revolutionary"

Last April

L. Pause et al, Optica 11 (2024) 2222

222 Vol. 11, No. 2 / February 2024 / *Optica* **Research Article**

OPTICA

Supercharged two-dimensional tweezer array with more than 1000 atomic qubits

LARS PAUSE,[1] LUKAS STURM,[1] MARCEL MITTENBÜHLER,[1] STEPHAN AMANN,[1,2] TILMAN PREUSCHOFF,[1] DOMINIK SCHÄFFNER,[1] MALTE SCHLOSSER,[1] AND GERHARD BIRKL[1,*]

[1]Technische Universität Darmstadt, Institut für Angewandte Physik, Schlossgartenstraße 7, 64289 Darmstadt, Germany
[2]Current address: Max-Planck-Institut für Quantenoptik, Hans-Kopfermann-Straße 1, 85748 Garching, Germany
*apqpub@physik.tu-darmstadt.de

Received 16 November 2023; revised 12 January 2024; accepted 19 January 2024; published 7 February 2024

We report on the realization of a large-scale quantum-processing architecture surpassing the tier of 1000 atomic qubits. By tiling multiple microlens-generated tweezer arrays, each operated by an independent laser source, we can eliminate laser-power limitations in the number of allocatable qubits. Already with two separate arrays, we implement combined 2D configurations of 3000 qubit sites with a mean number of 1167(46) single-atom quantum systems. The transfer of atoms between the two arrays is achieved with high efficiency. Thus, supercharging one array designated as the quantum

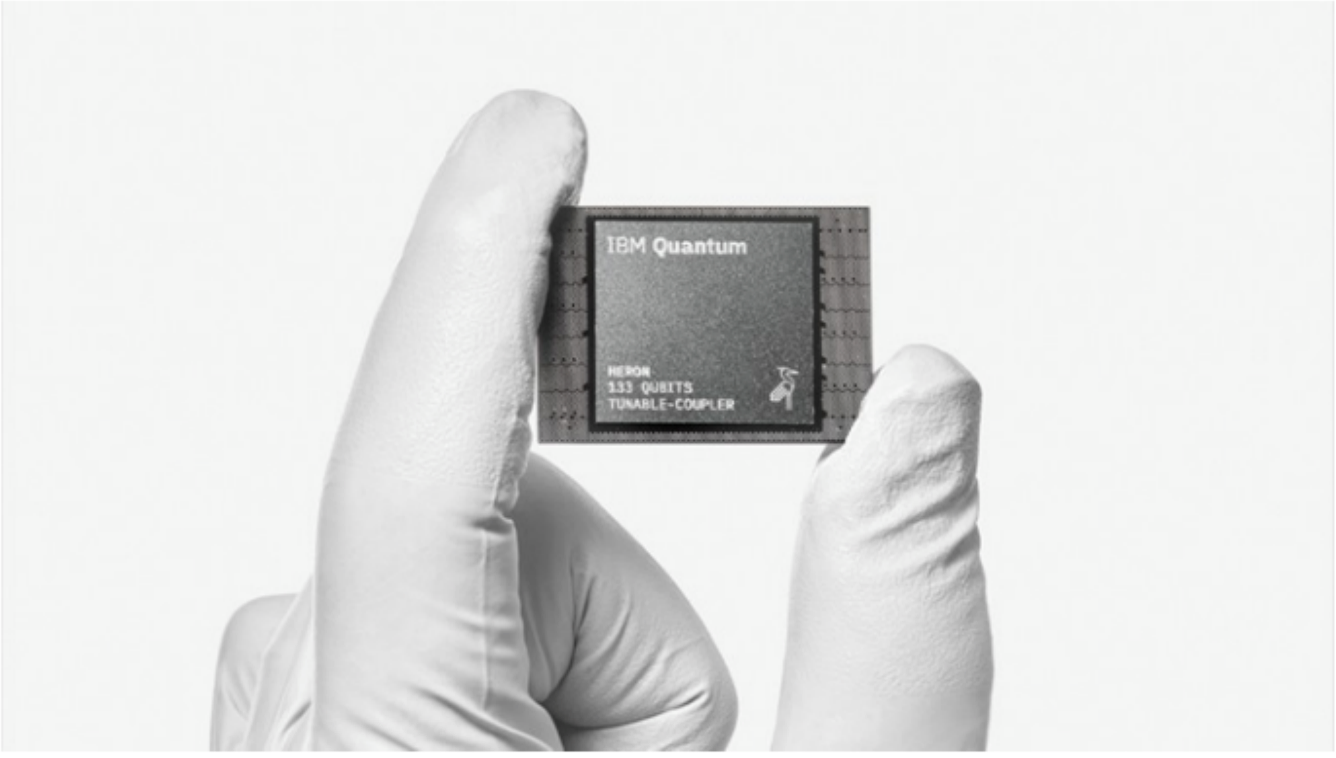

In its latest quantum processor, called Heron, IBM has improved the reliability of the qubits. Credit: Ryan Lavine for IBM

IBM has unveiled the first quantum computer with more than 1,000 qubits — the equivalent of the digital bits in an ordinary computer. But the company says that it will now shift gears and focus on making its machines more error-resistant rather than larger.

IBM, Nature 624 (2023) 238

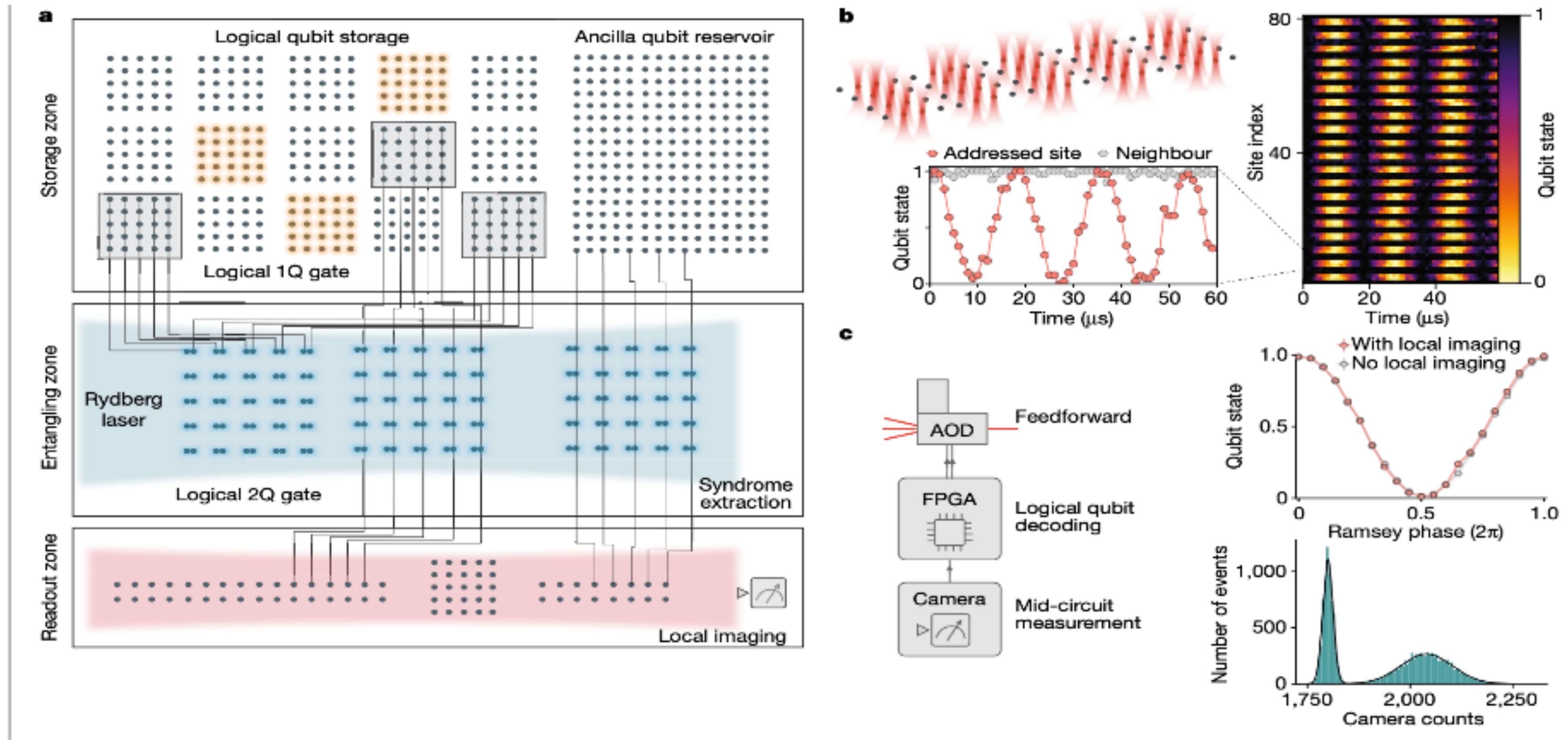

Fig. 1 | A programmable logical processor based on reconfigurable atom arrays. **a**, Schematic of the logical processor, split into three zones: storage, entangling and readout (see Extended Data Fig. 1 for detailed layout). Logical single-qubit and two-qubit operations are realized transversally with efficient, parallel operations. Transversal CNOTs are realized by interlacing two logical qubit grids and performing a single global entangling pulse that excites atoms to Rydberg states. Physical qubits are encoded in hyperfine ground states of ^{87}Rb atoms trapped in optical tweezers. **b**, Fully programmable single-qubit rotations are implemented using Raman excitation through a 2D AOD; parallel grid illumination delivers the same instruction to multiple atomic qubits. **c**, Mid-circuit readout and feedforward. The imaging histogram shows high-fidelity state discrimination (500 µs imaging time, readout fidelity approximately 99.8%; Methods) and the Ramsey fringe shows that qubit coherence is unaffected by measuring other qubits in the readout zone (error probability $p \approx 10^{-3}$; Methods). The FPGA performs real-time image processing, state decoding and feedforward (Fig. 4).

D. Bluvstein et al, Nature 626 (2024) 58

Last December


Willow's
Superconducting
Qubits
Willow's
Qubit Grid
105 Qubits

nature

https://doi.org/10.1038/s41586-024-08449-y

Accelerated Article Preview

Quantum error correction below the surface code threshold

Received: 24 August 2024

Accepted: 25 November 2024

Accelerated Article Preview

Cite this article as: Google Quantum AI and Collaborators. Quantum error correction below the surface code threshold. *Nature* https://doi.org/10.1038/s41586-024-08449-y (2024)

Google Quantum AI and Collaborators

This is a PDF file of a peer-reviewed paper that has been accepted for publication. Although unedited, the content has been subjected to preliminary formatting. Nature is providing this early version of the typeset paper as a service to our authors and readers. The text and figures will undergo copyediting and a proof review before the paper is published in its final form. Please note that during the production process errors may be discovered which could affect the content, and all legal disclaimers apply.

CLE PREVIEW

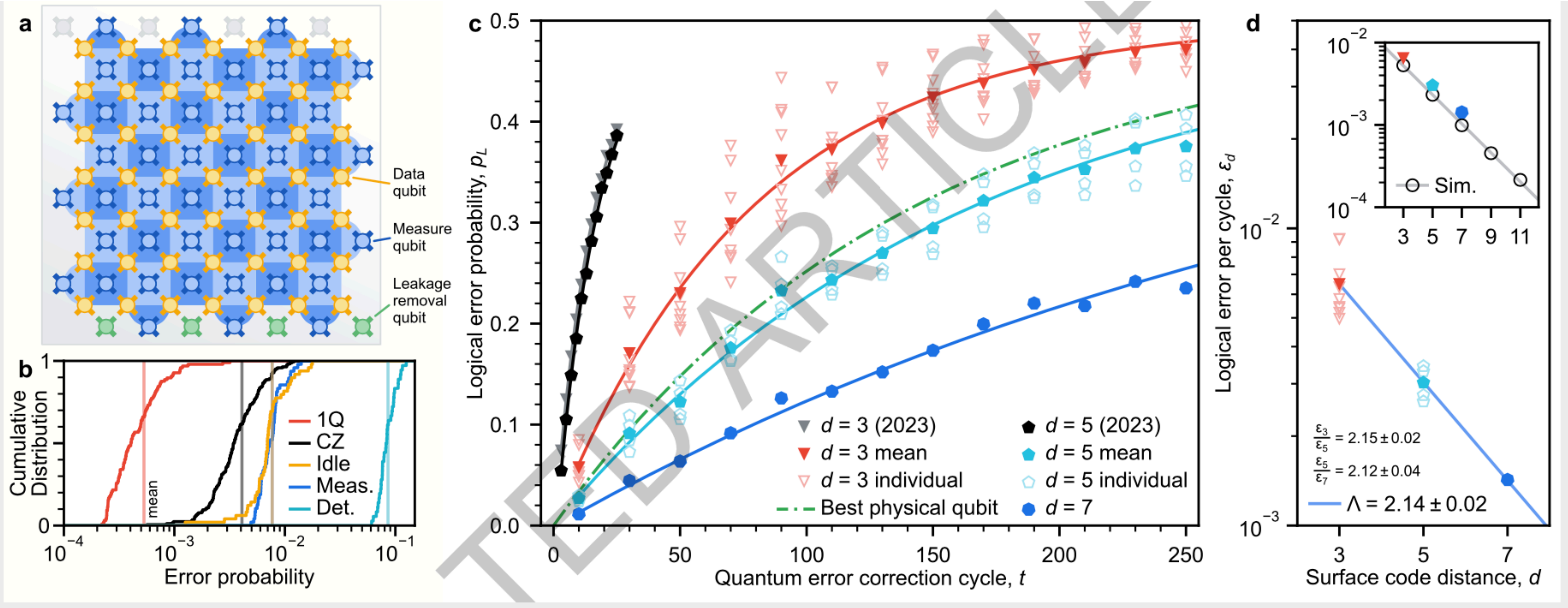

a
Data qubit
Measure qubit
Leakage removal qubit
b
Cumulative Distribution
mean
1Q
CZ
Idle
Meas.
Det.
Error probability
c
Logical error probability, p_L
Quantum error correction cycle, t
d = 3 (2023)
d = 3 mean
d = 3 individual
Best physical qubit
d = 5 (2023)
d = 5 mean
d = 5 individual
d = 7
d
Logical error per cycle, ε_d
Surface code distance, d
Sim.
$\frac{\varepsilon_3}{\varepsilon_5} = 2.15 \pm 0.02$
$\frac{\varepsilon_5}{\varepsilon_7} = 2.12 \pm 0.04$
$\Lambda = 2.14 \pm 0.02$
TED ARTICLE

Can Quantum Computer do better?

than what?

in which aspects?

Caveat!

- Any algorithmic process can be simulated efficiently using a Turing machine
- Any algorithmic process can be simulated efficiently using a probabilistic Turing machine
- Can universal quantum computer simulate efficiently an arbitrary physical system?

- QC is better than classical DC in classical problems?

combinatoric problem, $N! \simeq e^{N \ln N - N}$

- QC is better than classical DC in quantum problems?

parallelism, superposition, entanglement

!?

??

YouTube KR

Search

Create

AI for Science with Sir Paul Nurse, Demis Hassabis, Jennifer Doudna, and John Jumper

Google DeepMind
534K subscribers

Subscribe

2.2K | Share | Clip | Save

81K views 1 month ago Google DeepMind: The Podcast

All | From Google DeepMind | Demis Hassabis

Physicists Say They Know How Cold Fusion Works
Sabine Hossenfelder
175K views • 9 hours ago
New

윤건영 "尹, 이제 묵비권? 잡범의 길 가겠다는 것"
CBS 김현정의 뉴스쇼
2.6K views • 21 minutes ago
New

Starship Launch IMMINENT: What's wrong with SpaceX's...
What about it!?
294K views • 10 hours ago
New

I Believe The Universe Might Be Able To Think.
Sabine Hossenfelder
347K views • 2 days ago
New

[인터뷰] 궤도의 한방정리 "양자 컴퓨터... 젠슨황 말 맞나?"
CBS 김현정의 뉴스쇼
150K views • 1 day ago
New

5 BEST Things I Saw in Vegas at CES 2025
Undecided with Matt Ferrell
206K views • 12 hours ago

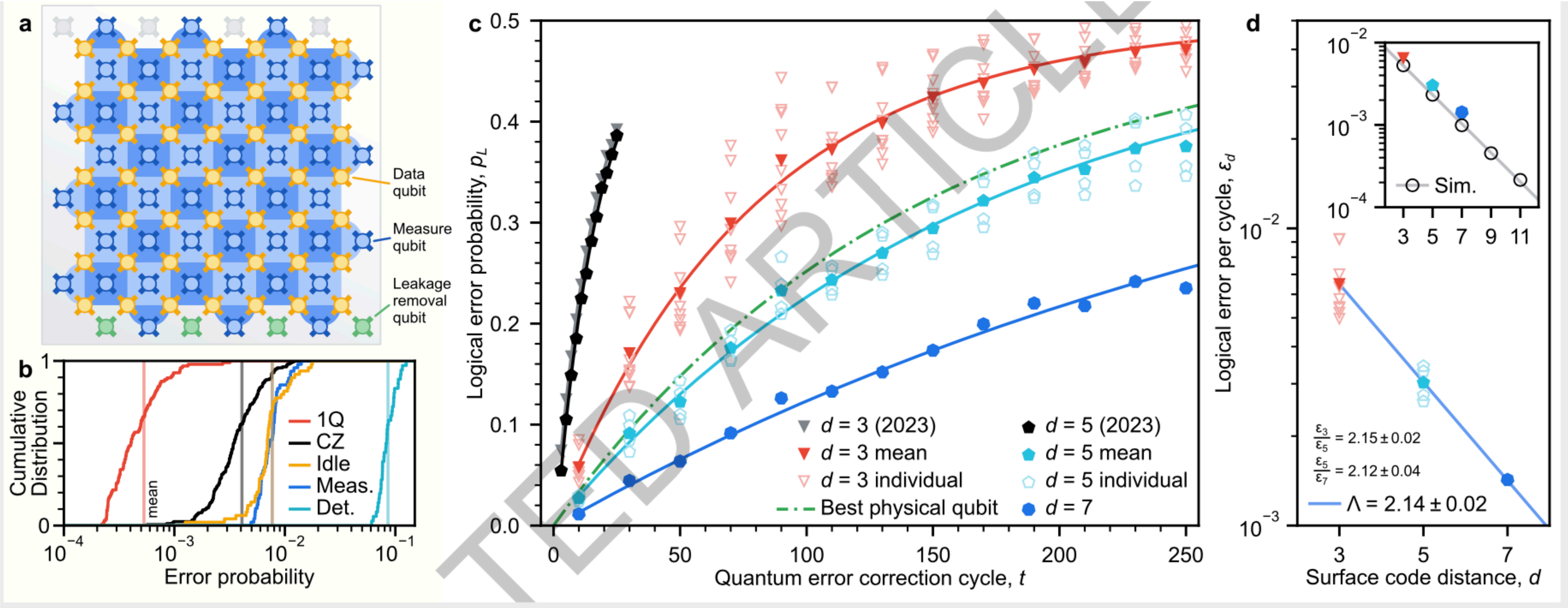

a
Data qubit
Measure qubit
Leakage removal qubit
b
Cumulative Distribution
mean
1Q
CZ
Idle
Meas.
Det.
Error probability
c
Logical error probability, p_L
d = 3 (2023)
d = 3 mean
d = 3 individual
Best physical qubit
d = 5 (2023)
d = 5 mean
d = 5 individual
d = 7
Quantum error correction cycle, t
d
Logical error per cycle, ε_d
Sim.
$\frac{\varepsilon_3}{\varepsilon_5} = 2.15 \pm 0.02$
$\frac{\varepsilon_5}{\varepsilon_7} = 2.12 \pm 0.04$
$\Lambda = 2.14 \pm 0.02$
Surface code distance, d

Quantum Computing in "noisy environment" or Fault–Tolerant QC

- Fighting quantum decoherence with entanglement
- Quantum Error Correction (QEC)

cf. B.M Terhal, Rev. Mod. Phys. 87 (2015) 307

Fault-Tolerant Quantum Memory

Nature 627 (2024) 778

Article

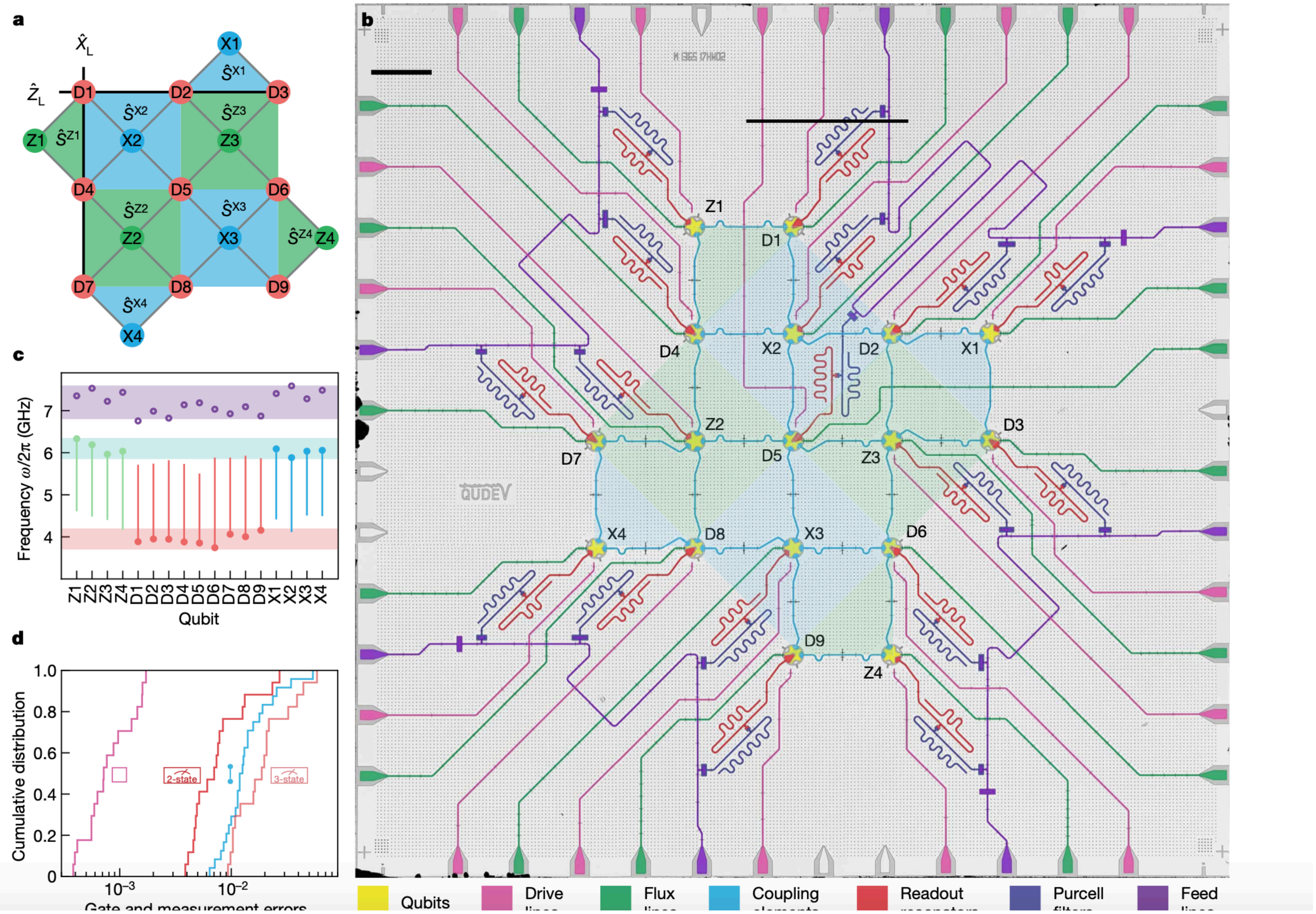

Fault-Tolerant Universal Quantum Gate

Nature 605 (2022) 675

Article

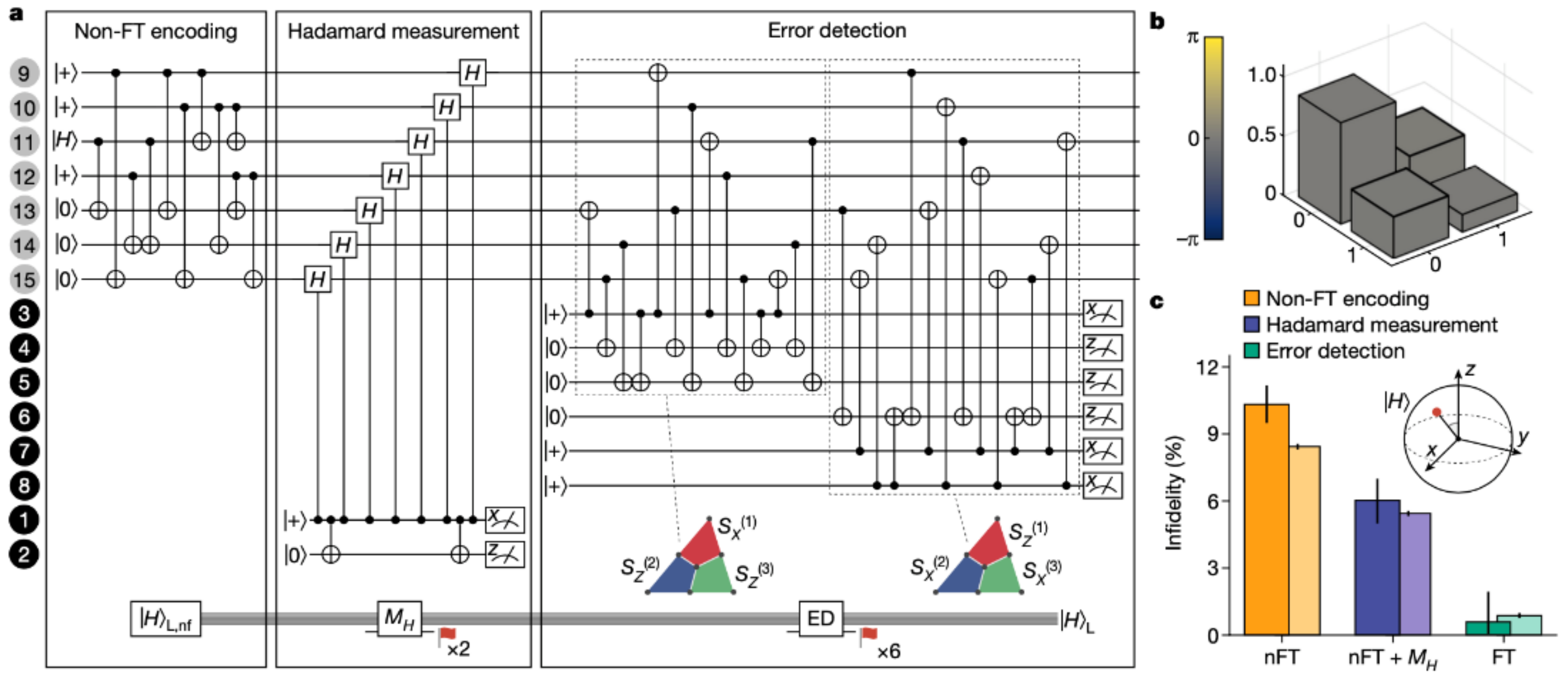

Fig. 4 | Fault-tolerant generation of a logical magic state $|H\rangle_L$. a, The magic state is prepared non-fault-tolerantly in a first step, where a physical magic state $|H\rangle$ is mapped to the logical state $|H\rangle_{L,nf}$ encoded in the data qubits at positions 9 to 15 in the ion string (see labels at left of circuit). Thereafter, a FT measurement of the Hadamard operator (M_H) is carried out. Two auxiliary qubits herald that the prepared state is a +1 eigenstate of the Hadamard operator but also that no dangerous error occurred during the measurement. The magic-state preparation is concluded with an error-detection (ED) block that measures the three X-type and Z-type stabilizers each in an FT fashion. The first part of the error-detection circuit (first dashed box), measures $S_X^{(1)}$, $S_Z^{(2)}$ and $S_Z^{(3)}$, whereas the second part measures $S_Z^{(1)}$, $S_X^{(2)}$ and $S_X^{(3)}$. The magic-state preparation is discarded and repeated in case of a non-trivial syndrome of the eight auxiliary qubits 1 to 8. **b**, Logical state tomography (see 'Transversal fault-tolerant operations') after FT magic-state preparation. The phase of the complex amplitudes is encoded in the colour of the three-dimensional bar plot and the wireframes depict ideal results. Phase deviations from the ideal density matrix are smaller than 50 mrad whereas amplitude deviations are smaller than 0.007. **c**, The decrease in infidelity of the logical magic state (red marker on Bloch sphere) after each step of the FT preparation procedure is observed experimentally and captured by depolarizing noise simulations (experimental and simulation results depicted darker and lighter, respectively).

Contents

1. Introduction on Quantum Error Correction (QEC)
2. QEC and Statistical Mechanics Model
3. Surface/Toric code and Z(2) Lattice Models (arXiv: 2412.14004)
4. Result and Discussion

My Background

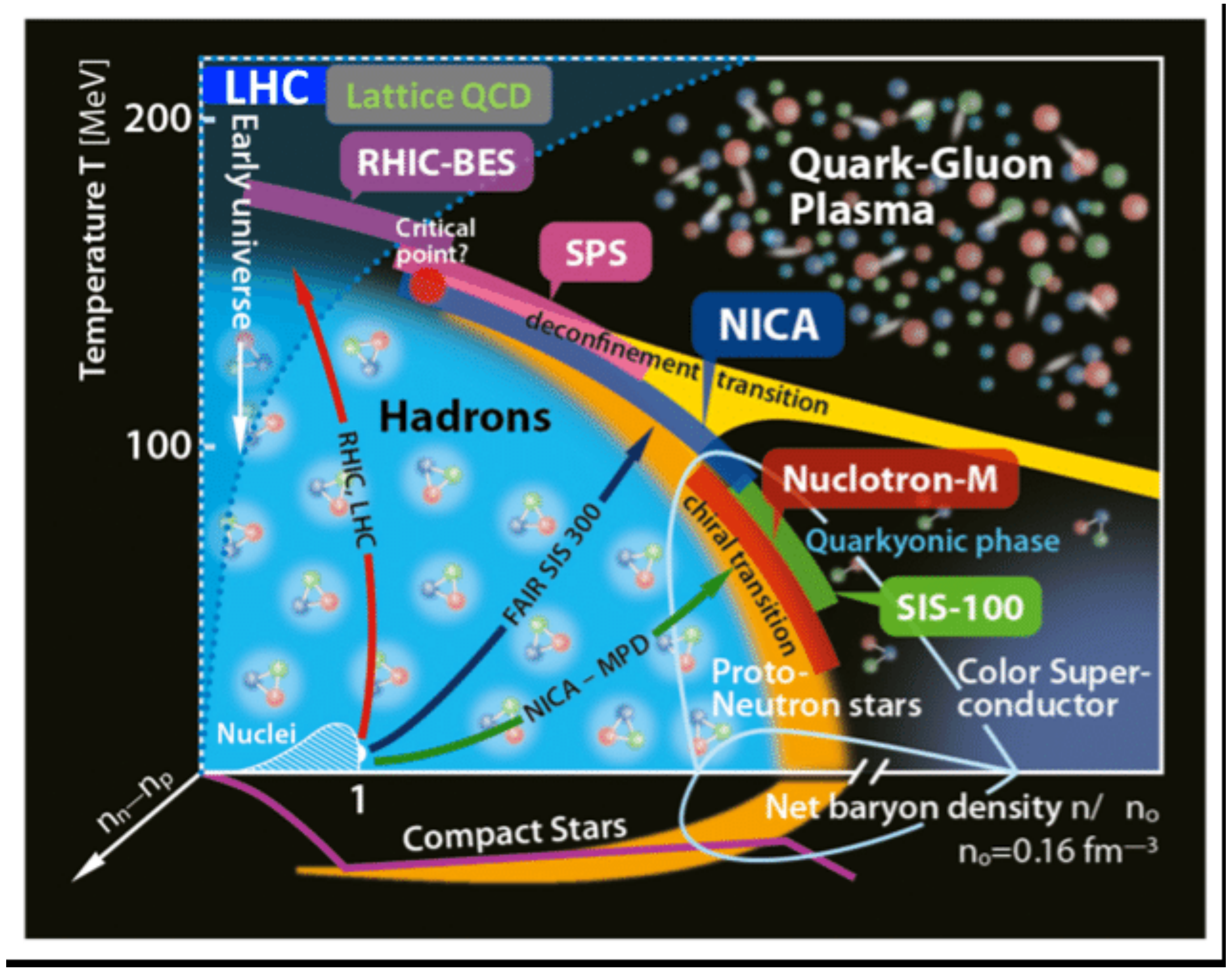

arXiv.2201.00202

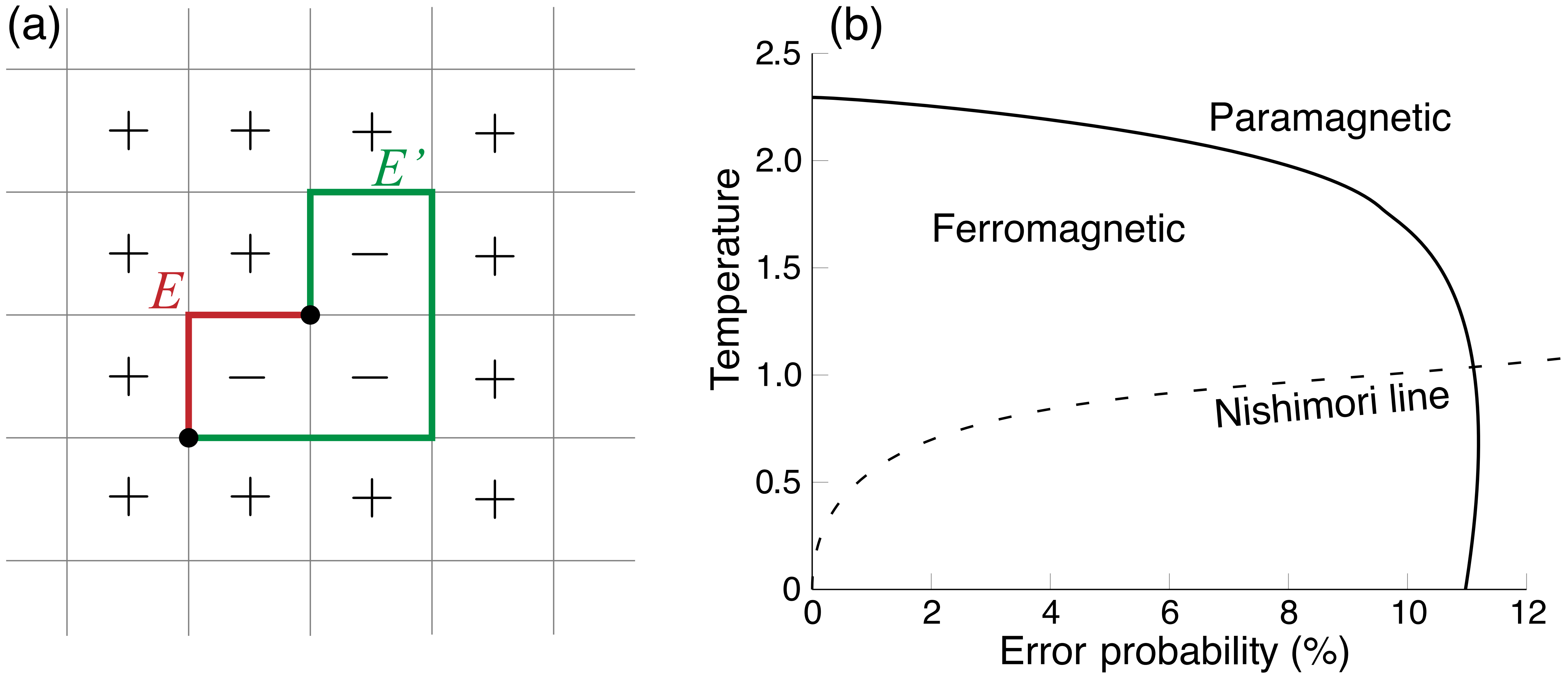

arXiv.2412.14004

1. Introduction on Quantum Error Correction

QEC: Shor's code (classical counter-part)

- Smallest classical code, $|0>_L = |000>$, $|1>_L = |111>$
- Measure each bit and do majority choice
- Not applicable to quantum computer
- cf. P. W. Shor, "Fault-tolerant quantum computation" in the proceedings of 37th FOCS, p55-65

QEC: Shor's code (9−bit concatenated code)

- $|0>_L = |000>$, $|1>_L = |111>$ (entangled qubits)
- Not measure data qubits, but measure parity of data without collapsing qubits supperposition/entanglement, $|\psi>_L = \cos\frac{\theta}{2}|0>_L + \sin\frac{\theta}{2}e^{\phi}|1>_L$
- Measuring any of qubits by Z_1, Z_2, Z_3 collapses entangled data qubits
- Measuring the ancilla qubit collapses entangled data qubits if 1 (or 2, or 3) data qubit is entangled with the ancilla qubit (i.e. measuring Z_1, or (Z_2, Z_3))
- Measuring ancilla qubit doesn't collapse entangled data qubits if 1,2 (or 2, 3) data qubits are entangled with the ancilla qubit (i.e. measuring Z_1Z_2, or Z_2Z_3)

Remind: Quantum Logic Gates

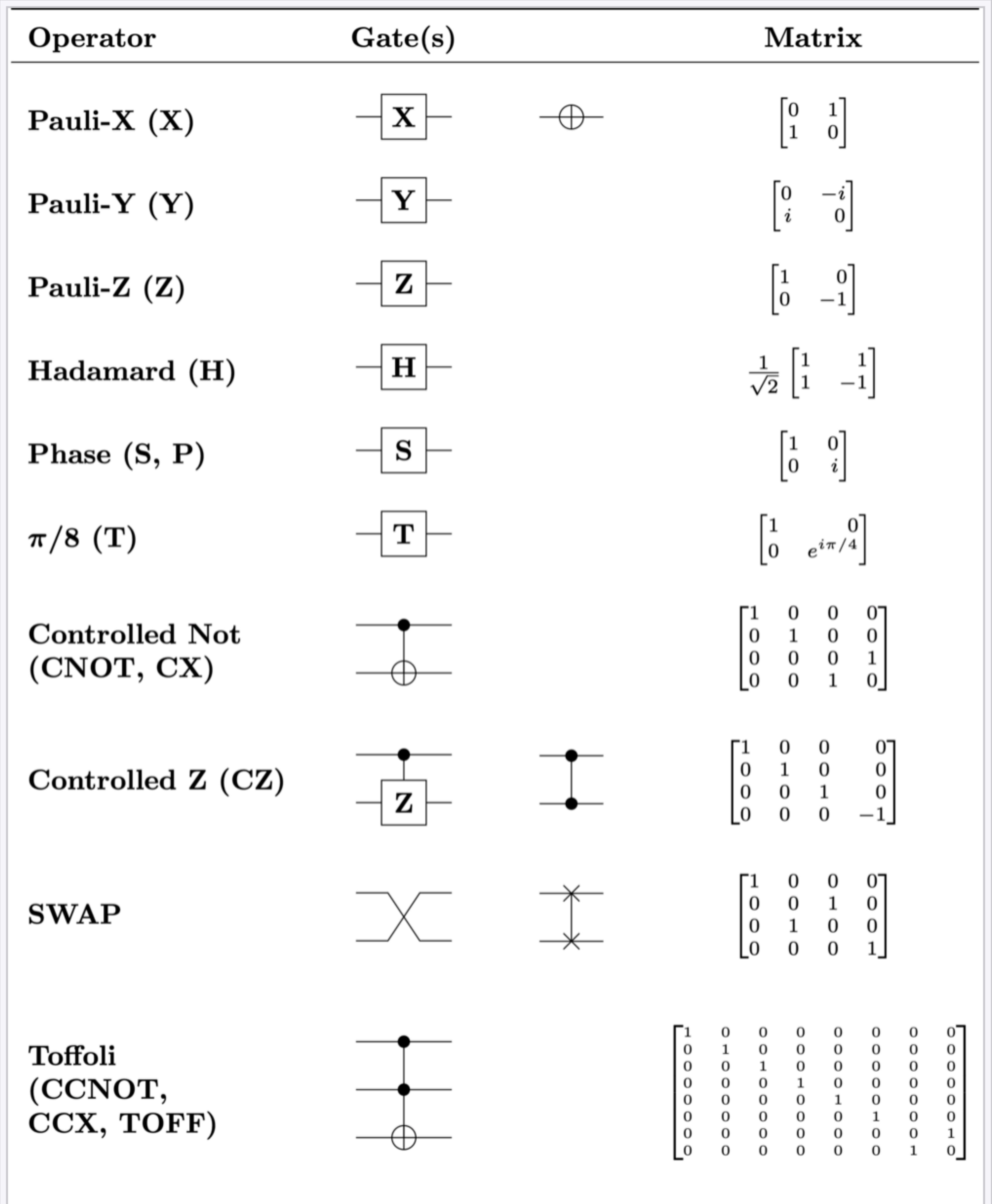

Operator	Gate(s)	Matrix
Pauli-X (X)	X	$\begin{bmatrix} 0 & 1 \\ 1 & 0 \end{bmatrix}$
Pauli-Y (Y)	Y	$\begin{bmatrix} 0 & -i \\ i & 0 \end{bmatrix}$
Pauli-Z (Z)	Z	$\begin{bmatrix} 1 & 0 \\ 0 & -1 \end{bmatrix}$
Hadamard (H)	H	$\frac{1}{\sqrt{2}}\begin{bmatrix} 1 & 1 \\ 1 & -1 \end{bmatrix}$
Phase (S, P)	S	$\begin{bmatrix} 1 & 0 \\ 0 & i \end{bmatrix}$
$\pi/8$ (T)	T	$\begin{bmatrix} 1 & 0 \\ 0 & e^{i\pi/4} \end{bmatrix}$
Controlled Not (CNOT, CX)		$\begin{bmatrix} 1 & 0 & 0 & 0 \\ 0 & 1 & 0 & 0 \\ 0 & 0 & 0 & 1 \\ 0 & 0 & 1 & 0 \end{bmatrix}$
Controlled Z (CZ)	Z	$\begin{bmatrix} 1 & 0 & 0 & 0 \\ 0 & 1 & 0 & 0 \\ 0 & 0 & 1 & 0 \\ 0 & 0 & 0 & -1 \end{bmatrix}$
SWAP		$\begin{bmatrix} 1 & 0 & 0 & 0 \\ 0 & 0 & 1 & 0 \\ 0 & 1 & 0 & 0 \\ 0 & 0 & 0 & 1 \end{bmatrix}$
Toffoli (CCNOT, CCX, TOFF)		$\begin{bmatrix} 1 & 0 & 0 & 0 & 0 & 0 & 0 & 0 \\ 0 & 1 & 0 & 0 & 0 & 0 & 0 & 0 \\ 0 & 0 & 1 & 0 & 0 & 0 & 0 & 0 \\ 0 & 0 & 0 & 1 & 0 & 0 & 0 & 0 \\ 0 & 0 & 0 & 0 & 1 & 0 & 0 & 0 \\ 0 & 0 & 0 & 0 & 0 & 1 & 0 & 0 \\ 0 & 0 & 0 & 0 & 0 & 0 & 0 & 1 \\ 0 & 0 & 0 & 0 & 0 & 0 & 1 & 0 \end{bmatrix}$

Common quantum logic gates by name (including abbreviation), circuit form(s) and the corresponding unitary matrices.

https://en.wikipedia.org/wiki/Quantum_logic_gate

$$i\frac{\partial}{\partial t}|\psi> = \hat{H}|\psi> \rightarrow |\psi(t)> = U(t)|\psi(0)>$$

$$U(t) = e^{-i\hat{H}t}$$

$$|\psi> = \prod_i \left(\cos\theta_i|0>_i + \sin\theta_i\, e^{i\phi_i}|1>_i\right)$$

Measurement (or Error)

$$\begin{pmatrix} 1 & 0 \\ 0 & -1 \end{pmatrix} \begin{pmatrix} 1 \\ 0 \end{pmatrix} = \begin{pmatrix} 1 \\ 0 \end{pmatrix} \longrightarrow Z|0> = |0>$$

$$\begin{pmatrix} 1 & 0 \\ 0 & -1 \end{pmatrix} \begin{pmatrix} 0 \\ 1 \end{pmatrix} = -\begin{pmatrix} 0 \\ 1 \end{pmatrix} \longrightarrow Z|1> = -|1>$$

$$\frac{1}{\sqrt{2}} \begin{pmatrix} 0 & 1 \\ 1 & 0 \end{pmatrix} \begin{pmatrix} 1 \\ 1 \end{pmatrix} = \frac{1}{\sqrt{2}} \begin{pmatrix} 1 \\ 1 \end{pmatrix} \longrightarrow X|+> = |+>$$

$$\frac{1}{\sqrt{2}} \begin{pmatrix} 0 & 1 \\ 1 & 0 \end{pmatrix} \begin{pmatrix} 1 \\ -1 \end{pmatrix} = -\frac{1}{\sqrt{2}} \begin{pmatrix} 1 \\ -1 \end{pmatrix} \longrightarrow X|-> = -|->$$

Measurement (or Error)

$$\begin{pmatrix} 0 & 1 \\ 1 & 0 \end{pmatrix} \begin{pmatrix} 1 \\ 0 \end{pmatrix} = \begin{pmatrix} 0 \\ 1 \end{pmatrix} \longrightarrow X|0> = |1>$$

$$\begin{pmatrix} 0 & 1 \\ 1 & 0 \end{pmatrix} \begin{pmatrix} 0 \\ 1 \end{pmatrix} = \begin{pmatrix} 1 \\ 0 \end{pmatrix} \longrightarrow X|1> = |0>$$

$$\frac{1}{\sqrt{2}} \begin{pmatrix} 1 & 0 \\ 0 & -1 \end{pmatrix} \begin{pmatrix} 1 \\ 1 \end{pmatrix} = \frac{1}{\sqrt{2}} \begin{pmatrix} 1 \\ -1 \end{pmatrix} \longrightarrow Z| + > = | - >$$

$$\frac{1}{\sqrt{2}} \begin{pmatrix} 1 & 0 \\ 0 & -1 \end{pmatrix} \begin{pmatrix} 1 \\ -1 \end{pmatrix} = \frac{1}{\sqrt{2}} \begin{pmatrix} 1 \\ 1 \end{pmatrix} \longrightarrow Z| - > = | + >$$

Hadamard

$$\frac{1}{\sqrt{2}}\begin{pmatrix}1 & 1\\ 1 & -1\end{pmatrix}\begin{pmatrix}1\\ 0\end{pmatrix} = \frac{1}{\sqrt{2}}\begin{pmatrix}1\\ 1\end{pmatrix} \longrightarrow \quad H|0> = |+>$$

$$\frac{1}{\sqrt{2}}\begin{pmatrix}1 & 1\\ 1 & -1\end{pmatrix}\begin{pmatrix}0\\ 1\end{pmatrix} = \frac{1}{\sqrt{2}}\begin{pmatrix}1\\ -1\end{pmatrix} \longrightarrow \quad H|1> = |->$$

$$\frac{1}{\sqrt{2}}\begin{pmatrix}1 & 1\\ 1 & -1\end{pmatrix}\begin{pmatrix}1\\ 1\end{pmatrix} = \begin{pmatrix}1\\ 0\end{pmatrix} \longrightarrow \quad H|+> = |0>$$

$$\frac{1}{\sqrt{2}}\begin{pmatrix}1 & 1\\ 1 & -1\end{pmatrix}\begin{pmatrix}1\\ -1\end{pmatrix} = \begin{pmatrix}0\\ 1\end{pmatrix} \longrightarrow \quad H|-> = |1>$$

Z Measurement effect

Before measurement

$$c_1|000> + c_2|111>$$

After measurement

$|000>$ or $|111>$ with probability $|c_1|^2$ or $|c_2|^2$

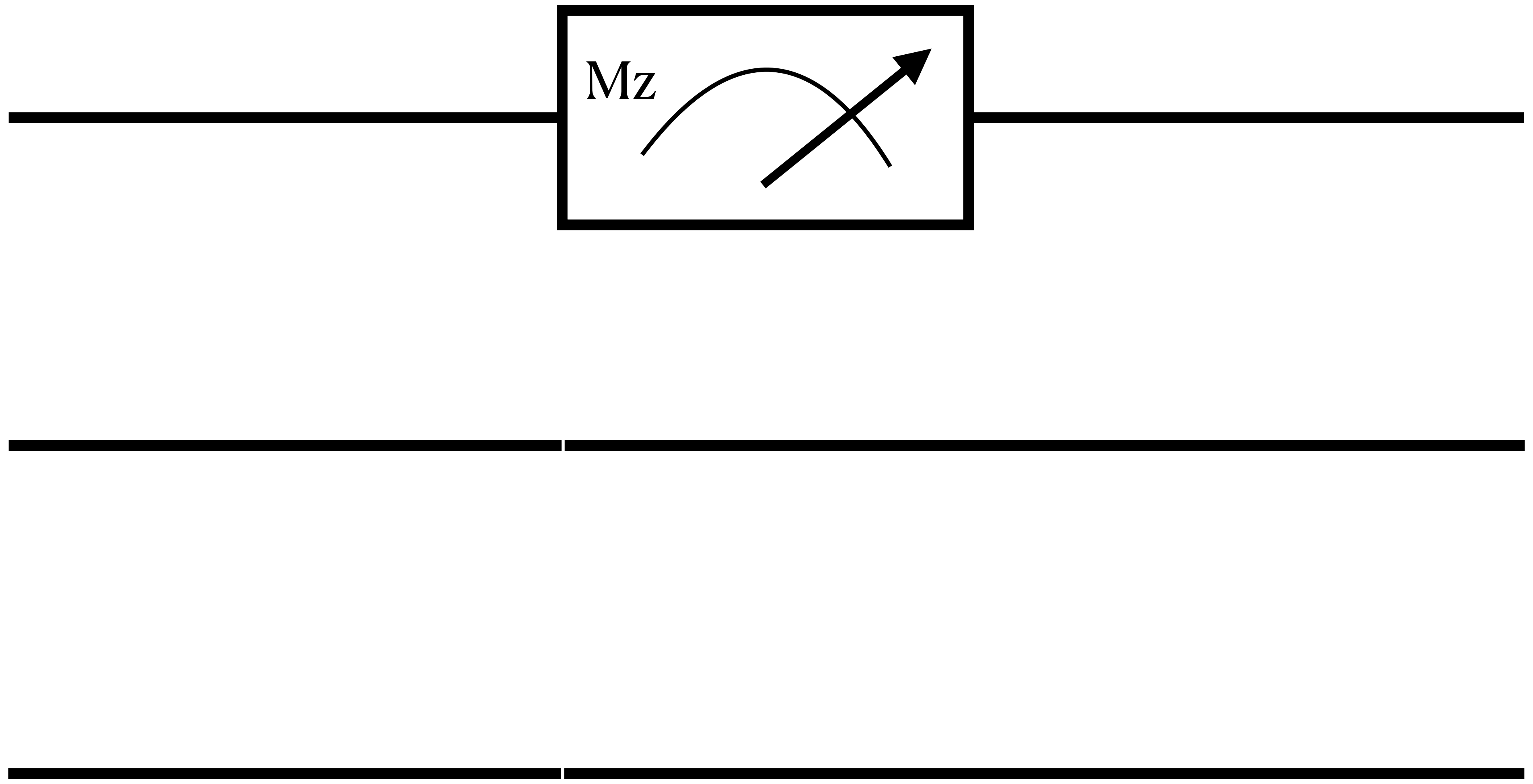

$Z_1 Z_2$ parity check

Before measurement

Surface/Toric code and QEC

Dennis, E., Kitaev, A., Landahl, A. and Preskill, J., 2002. Topological quantum memory. Journal of Mathematical Physics, 43(9), pp.4452–4505.

2-dimensional array of qubits: periodic boundary/open boundary = topological vs surface

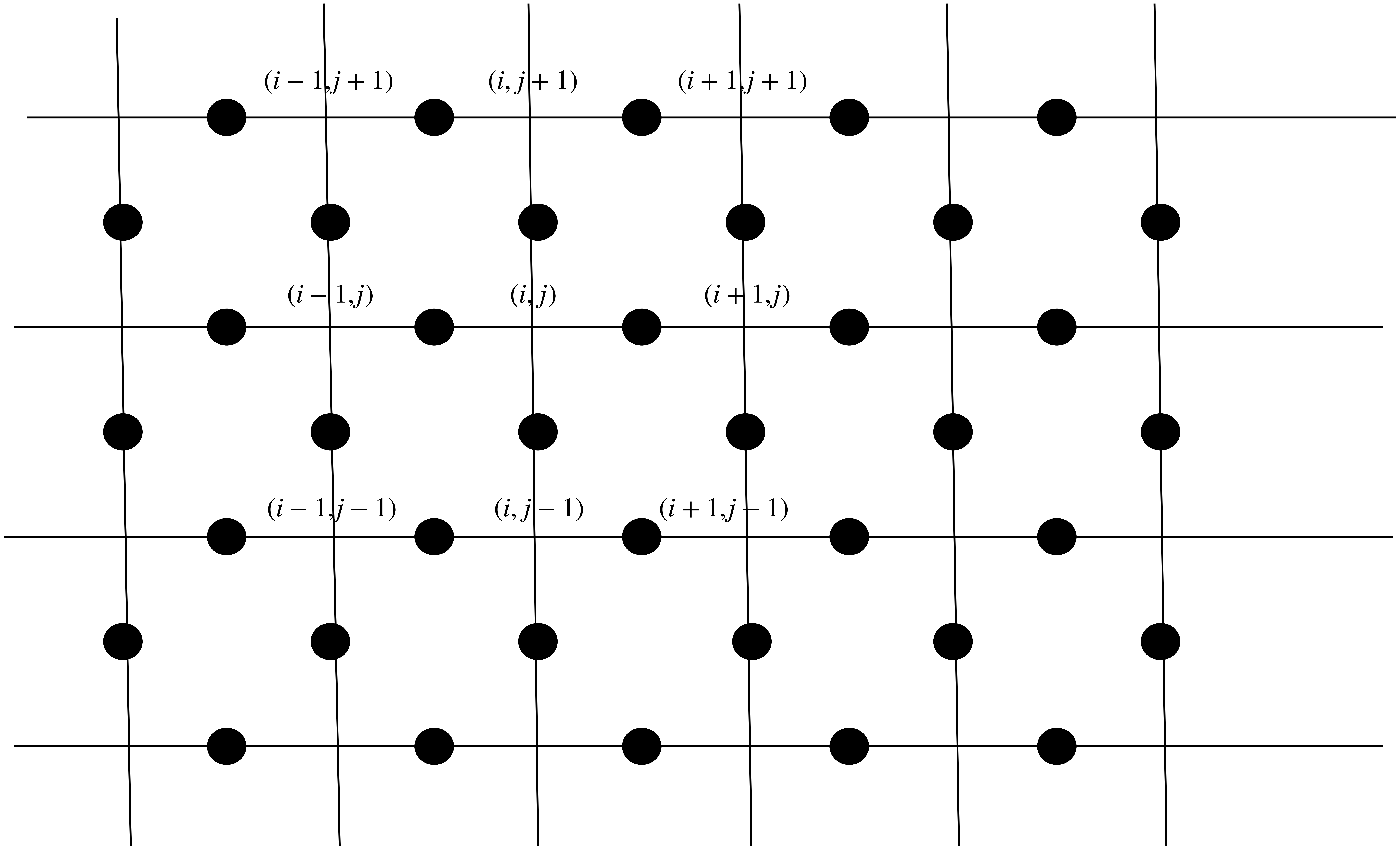

$$\hat{S}_X(i,j) = \hat{X}_1(i,j)\hat{X}_2(i,j)\hat{X}_1(i-1,j)\hat{X}_2(i-1,j)$$

$$\hat{S}_Z(i,j) = \hat{Z}_1(i,j)\hat{Z}_2(i,j)\hat{Z}_2(i+1,j)\hat{Z}_1(i,j+1)$$

$$|\psi>_L = \{\hat{S}|\psi> = +|\psi> \text{ for all } \hat{S}\}$$

1. $\hat{S}_X, \hat{S}_Z$ are called check operators of surface/Toric code or stabilizers of stabilizer code
2. $|\psi>_L$ is 2 logical qubit system
3. 4 logical operators, $\bar{X}_1, \bar{X}_2, \bar{Z}_1, \bar{Z}_2$ on $|\psi>_L$

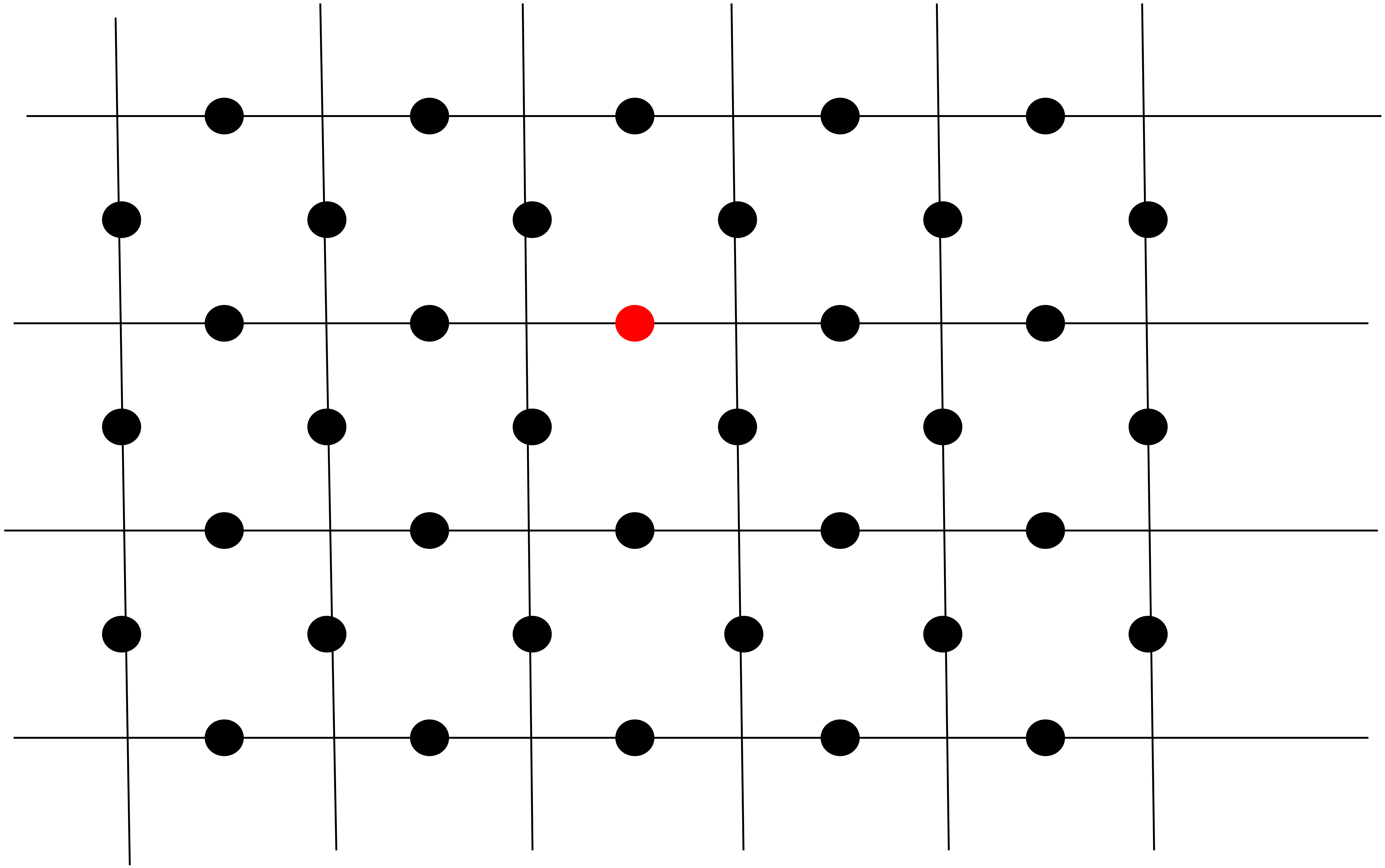

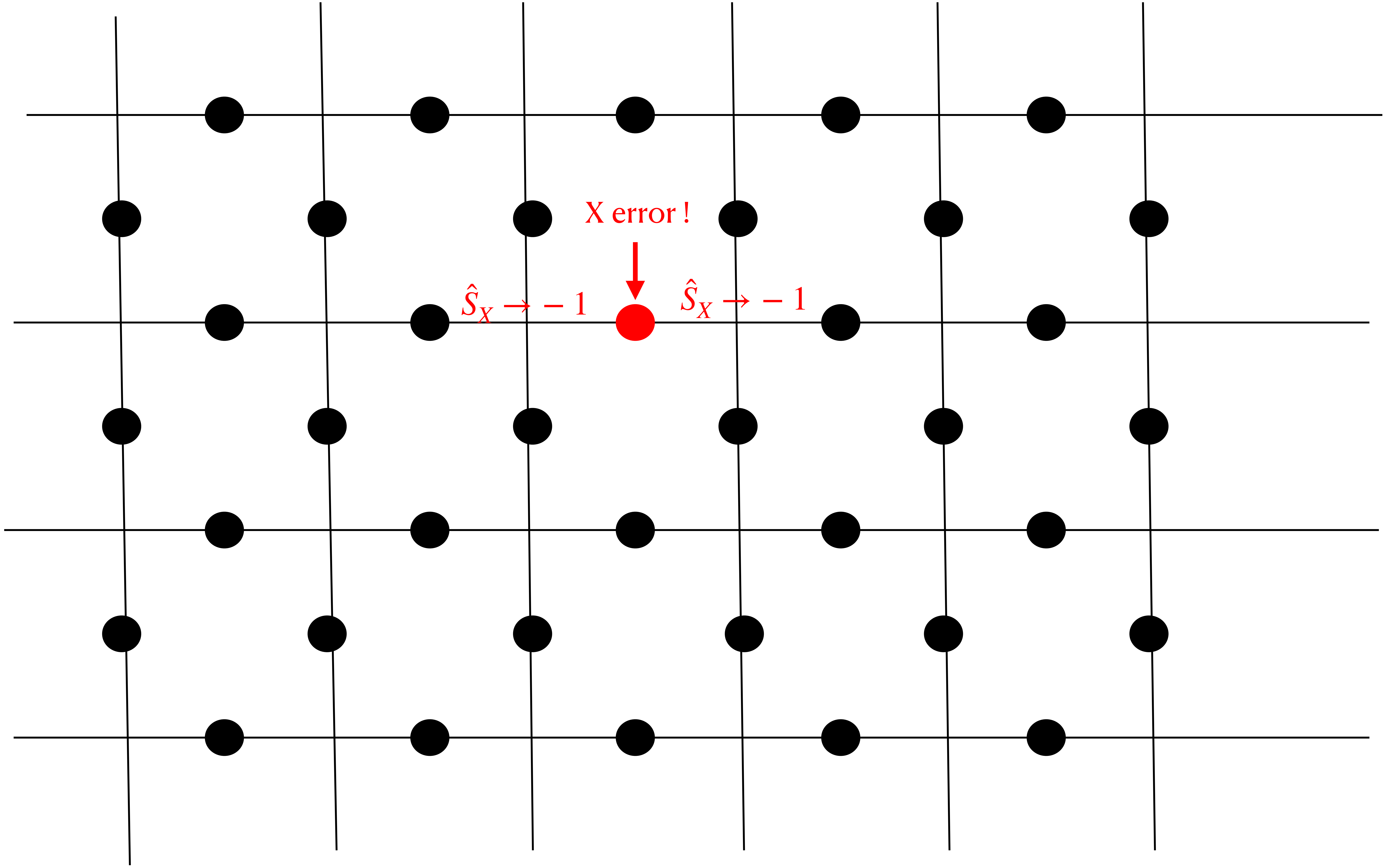
X error !
$\hat{S}_X \to -1$
$\hat{S}_X \to -1$

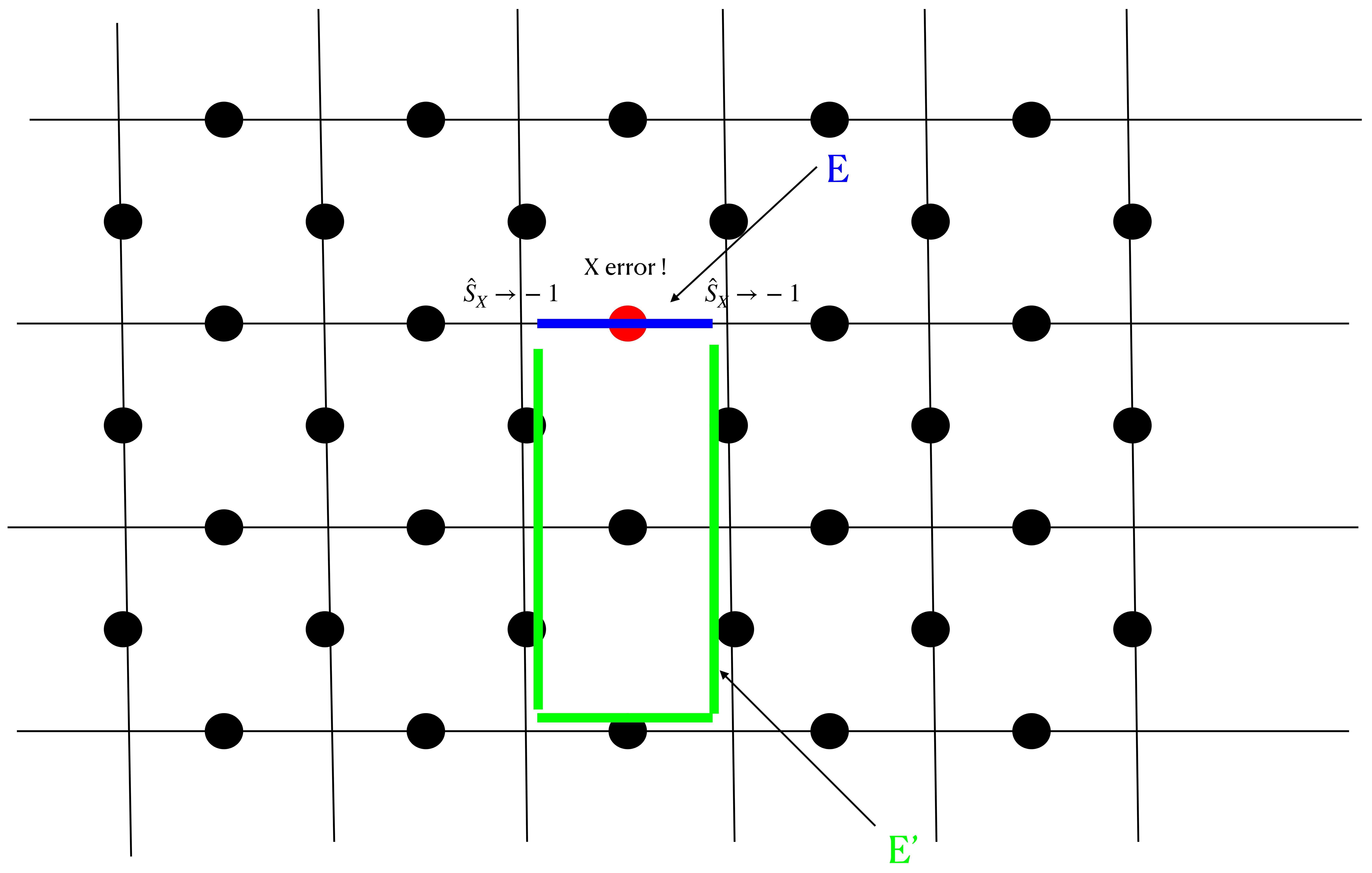

E
X error !
$\hat{S}_X \to -1$
$\hat{S}_X \to -1$
E'

- A given "syndrome", there are many equivalent error configurations which shares the same "boundary"
- For a given error configuration, E,

$$P(E) = \prod_l (1-p)^{1-n_E(l)} p^{n_E(l)} = \prod_l (1-p) \left(\frac{p}{1-p} \right)^{n_E(l)}$$

$$= \prod_l (1-p) \prod_l \left(\frac{p}{1-p} \right)^{n_E(l)}, \;\; n_E(l) = 1 \text{ for } l \in E, \;\; n_E(l) = 0 \text{ for } l \notin E$$

- For different configurations, E', where $E' = E + C$ (C is cycle) for a given E, consider $P(C)$
- If $n_C(l) = 1$ and $n_E(l) = 0$, then the link l belongs to E' (E is fixed).

$$P(C) = \prod_l (1-p) \prod_l \left(\frac{p}{1-p}\right)^{n_{E'}(l)} \propto \left(\frac{p}{1-p}\right)^{n_E(l)+n_C(l)} \propto \left(\frac{p}{1-p}\right)^{n_C(l)}$$

- If $n_C(l) = 1$ and $n_E(l) = 1$, then the link l doesn't belongs to E'.

$$P(C) \propto \left(\frac{1-p}{p}\right)^{n_C(l)}$$

- Thus $P(E'|E) \propto \prod_l exp(J_l u_l)$ with $u_l = 1 - 2n_C(l)$ where

$u_l \in \{-1,1\}$ (note that $u_l = 1$ if $n_C(l) = 0$, $u_l = -1$ if $n_C(l) = 1$) with

$$e^{-2j_l} = \frac{p}{1-p} \text{ for } l \notin E, \ = \frac{1-p}{p} \text{ for } l \in E$$

- Finding Solution for the constraint $\prod_{l \ni s} u_l = 1$ (S are the sites with

even number links on that site which have $u_l = -1$) is convenient

2. QEC and Statistical Mechanics Model

Statistical Mechanics Models: Dennis et al.

- Surface/Toric code with bit-flip noise or phase-flip noise (together with syndrome noise or without syndrome noise)
- In 2-D, solution for $\prod_{l \ni s} u_l = 1$ is random-bond Ising model
- In 3-D, solution for $\prod_{l \ni s} u_l = 1$ is Z(2) Plaquette Gauge Model
- "Probabilistic interpretation" is related to some statistical model

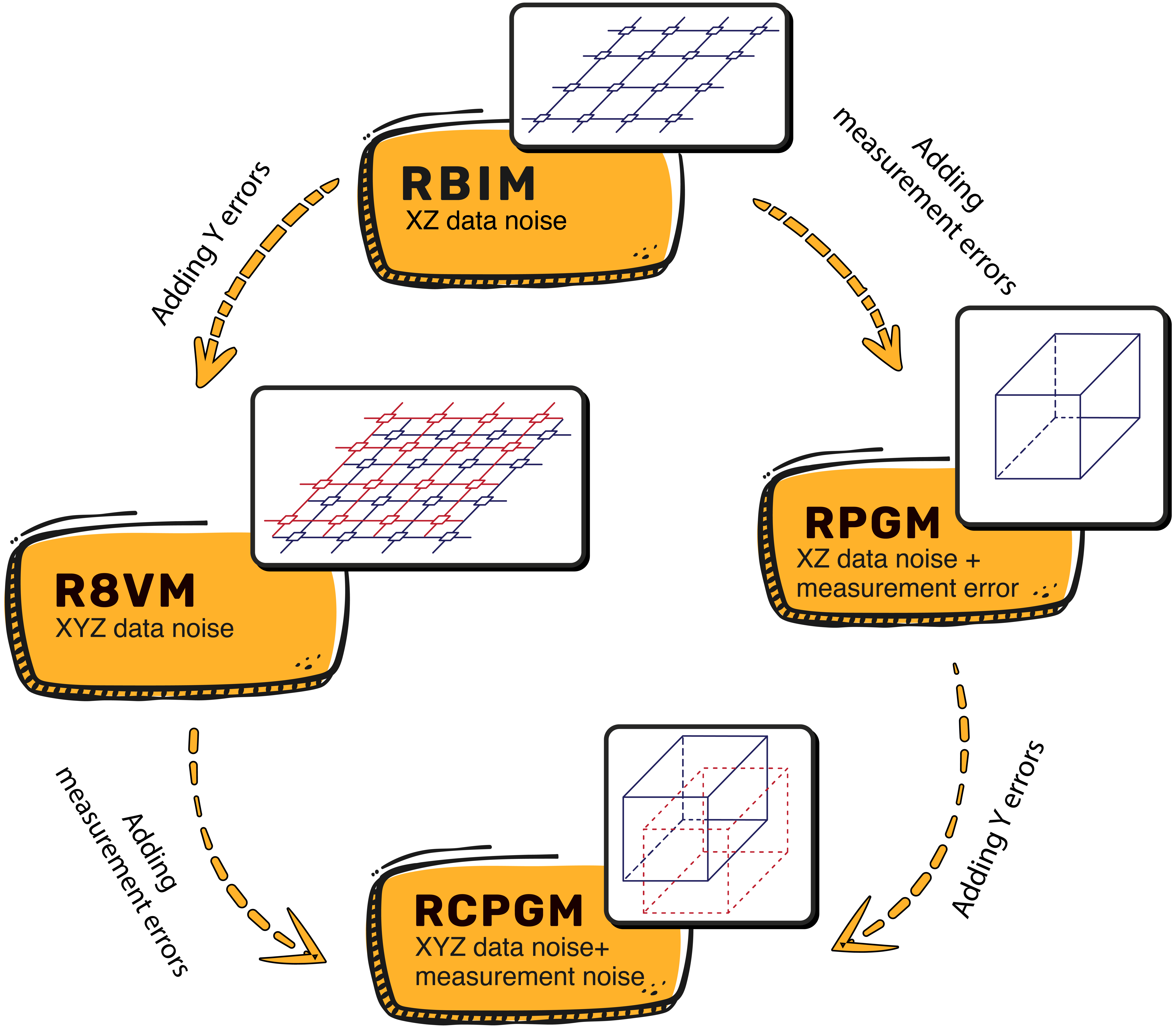
RBIM
XZ data noise
Adding measurement errors
RPGM
XZ data noise +
measurement error
Adding Y errors
RCPGM
XYZ data noise+
measurement noise
Adding measurement errors
R8VM
XYZ data noise
Adding Y errors

Quantum error and statistical model

- Specific quantum code with stabilizer formalism
- Modeling quantum error pattern
- Mapping quantum error pattern to statistical model
- cf. simple case: Dennis et al, J. Math. Phys. 43 (2002) 4452

Error rate and threshold probability

- If the quantum error rate is higher than the "threshold probability", QEC is not possible.
- Above the threshold probability, "probabilistic correction" is not possible.
- "Probabilistic interpretation" is related to some statistical model

3. Surface/Toric Code

and

Z(2) Lattice Models

(with M. Rispler, D. Vodola, M. Muller,

arXiv: 2412.14004)

Toric code circuit

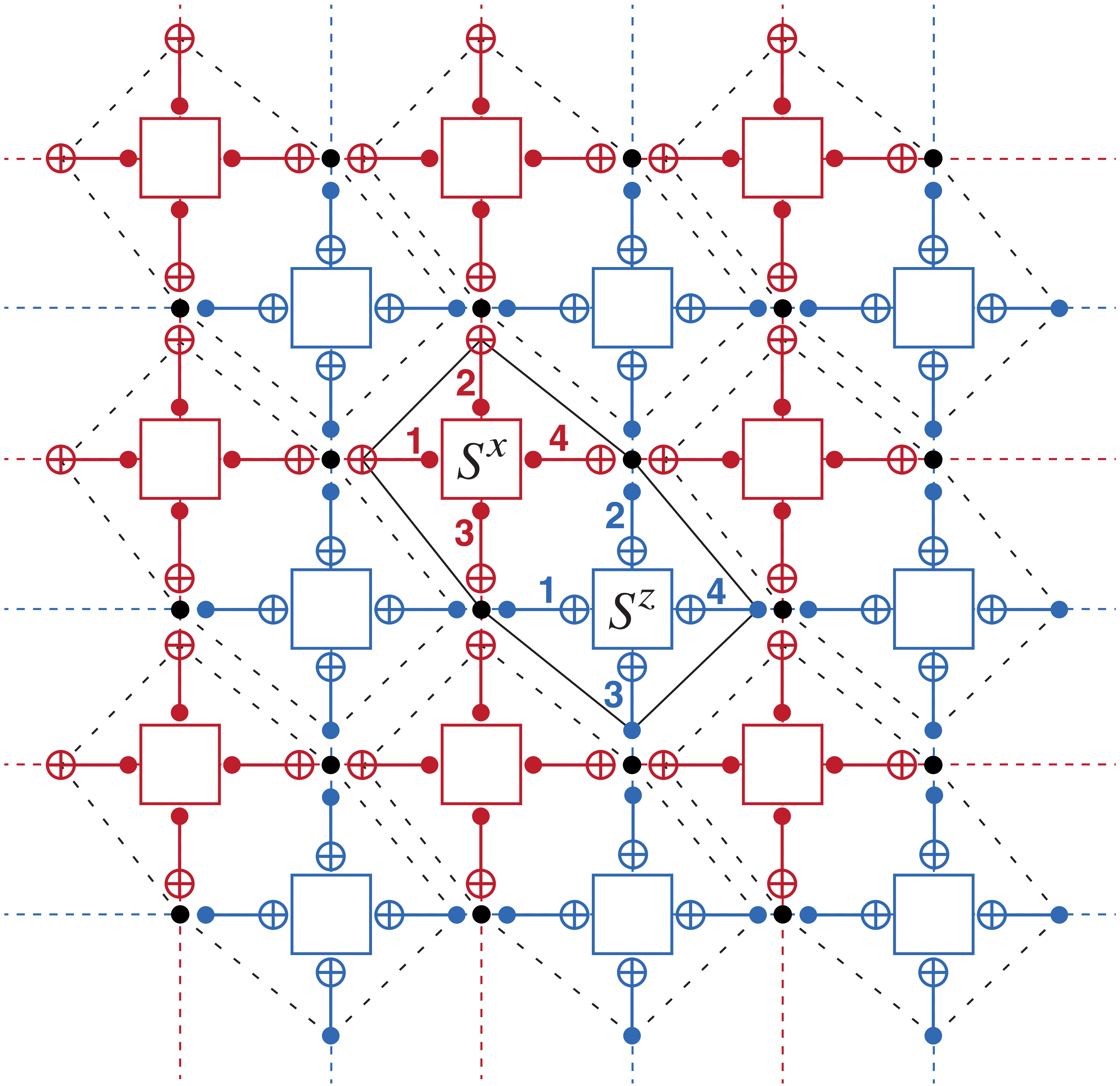

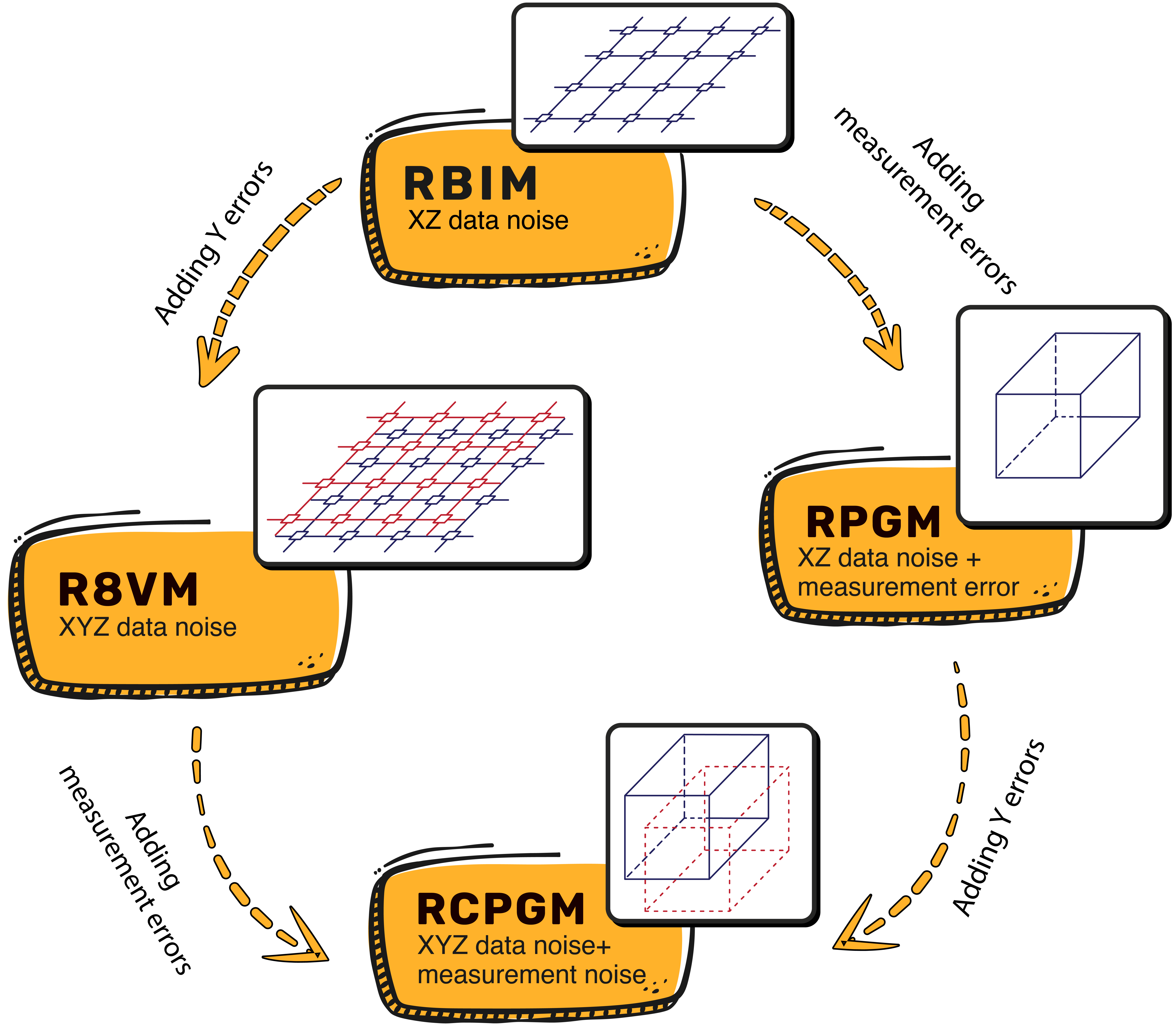
RBIM
XZ data noise
Adding Y errors
Adding measurement errors
R8VM
XYZ data noise
RPGM
XZ data noise + measurement error
Adding measurement errors
Adding Y errors
RCPGM
XYZ data noise+ measurement noise

Quantum Error Models and Mapped Statistical physics models in Toric Code

- Random bit flip (σ_x) error or phase flip (σ_z) error

  —〉 2-D Ising model with quenched anti-ferromagnetic coupling

- Random bit flip error or phase flip error + syndrome measurement error

  —〉 3-D $Z(2)$ gauge theory with quenched anti-ferromagnetic coupling

Quantum Error Models and Mapped Statistical physics models in Toric Code

- Independent (σ_x), (σ_z) error + syndrome measurement error

  —〉 3–D $Z(2)$ gauge theory

  with quenched anisotropic anti–ferromagnetic coupling

- Depolarizing (i.e., $(\sigma_x),(\sigma_y),(\sigma_z)$) error + syndrome measurement error

  —〉 3–D $Z(2) \times Z(2)$ gauge theory

  with anisotropic quenched anti–ferromagnetic coupling

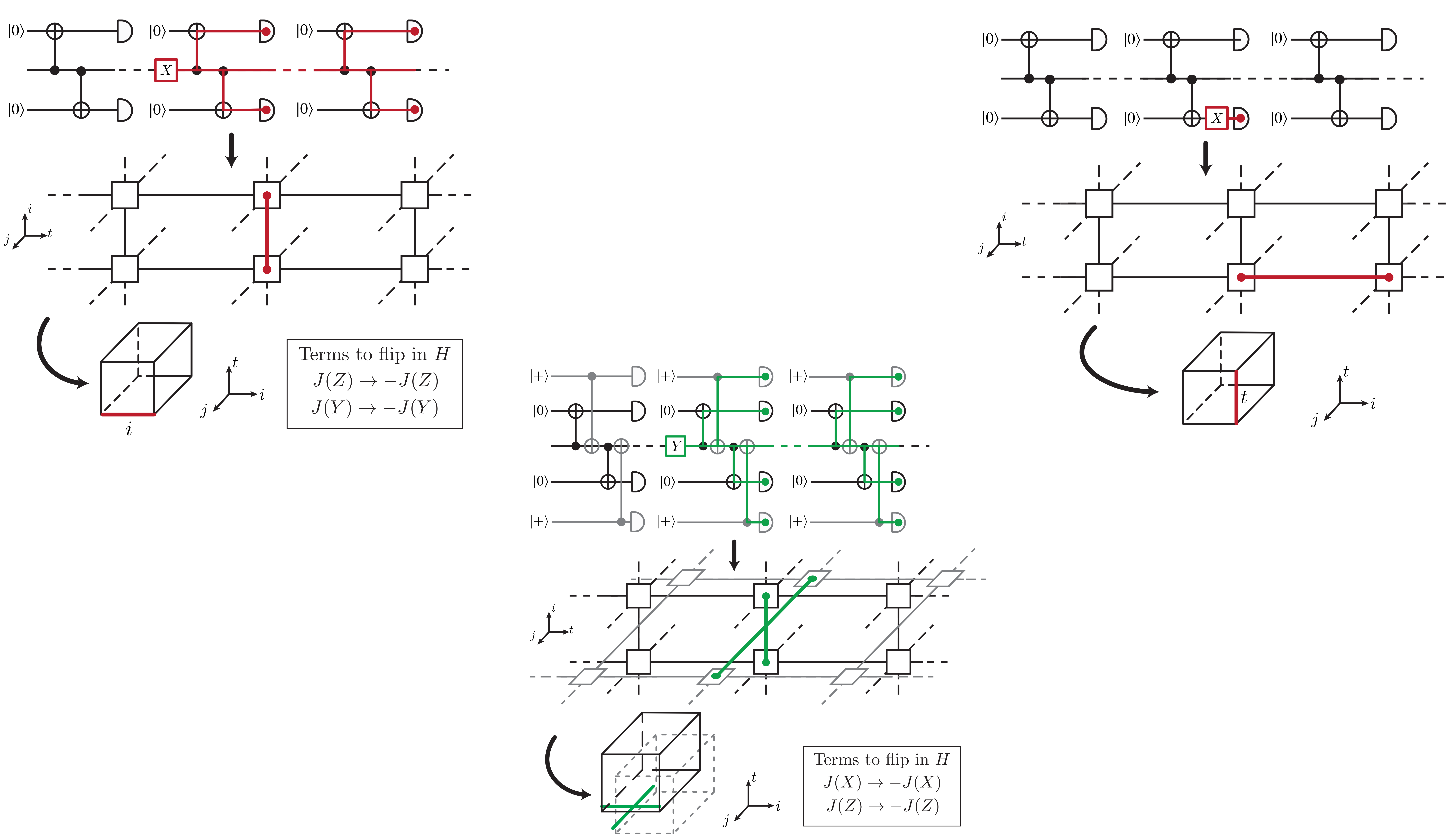

|0⟩
|+⟩
X
Y
i
j
t
Terms to flip in H
$J(Z) \to -J(Z)$
$J(Y) \to -J(Y)$
Terms to flip in H
$J(X) \to -J(X)$
$J(Z) \to -J(Z)$

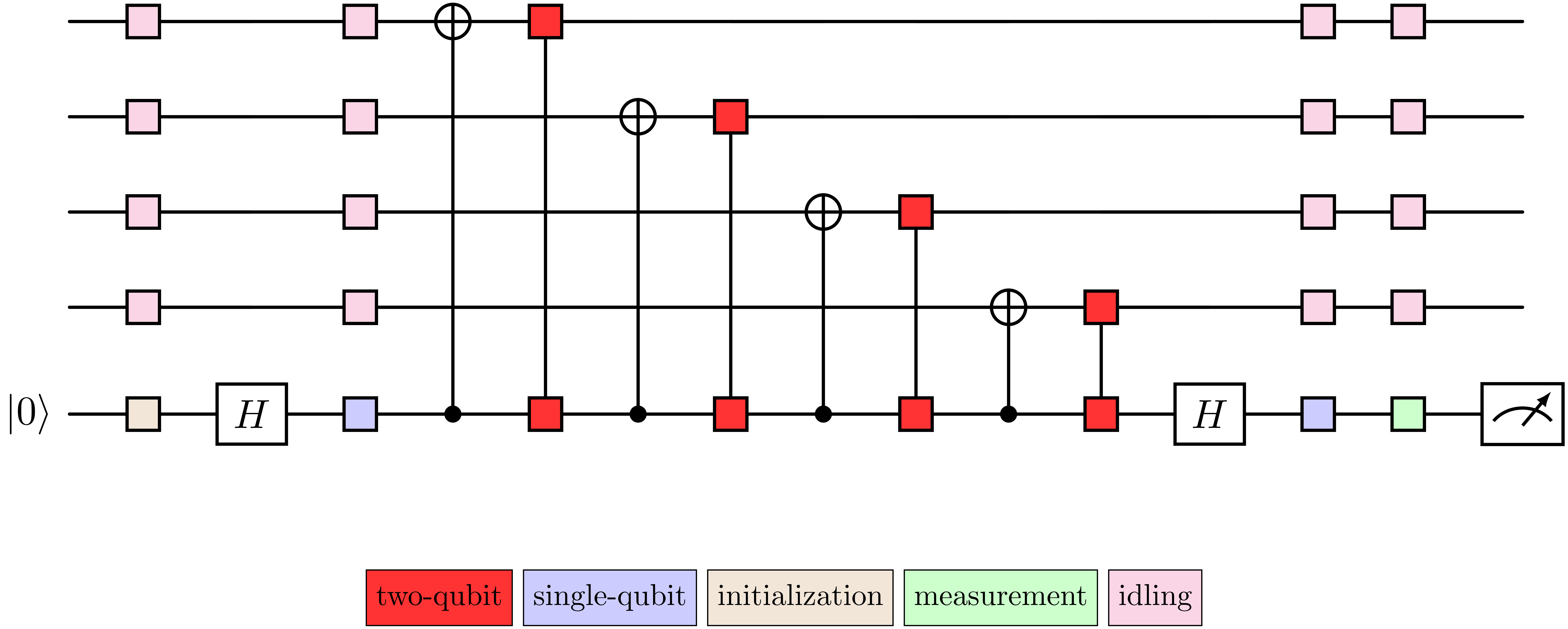

|0⟩
H
H
two-qubit
single-qubit
initialization
measurement
idling

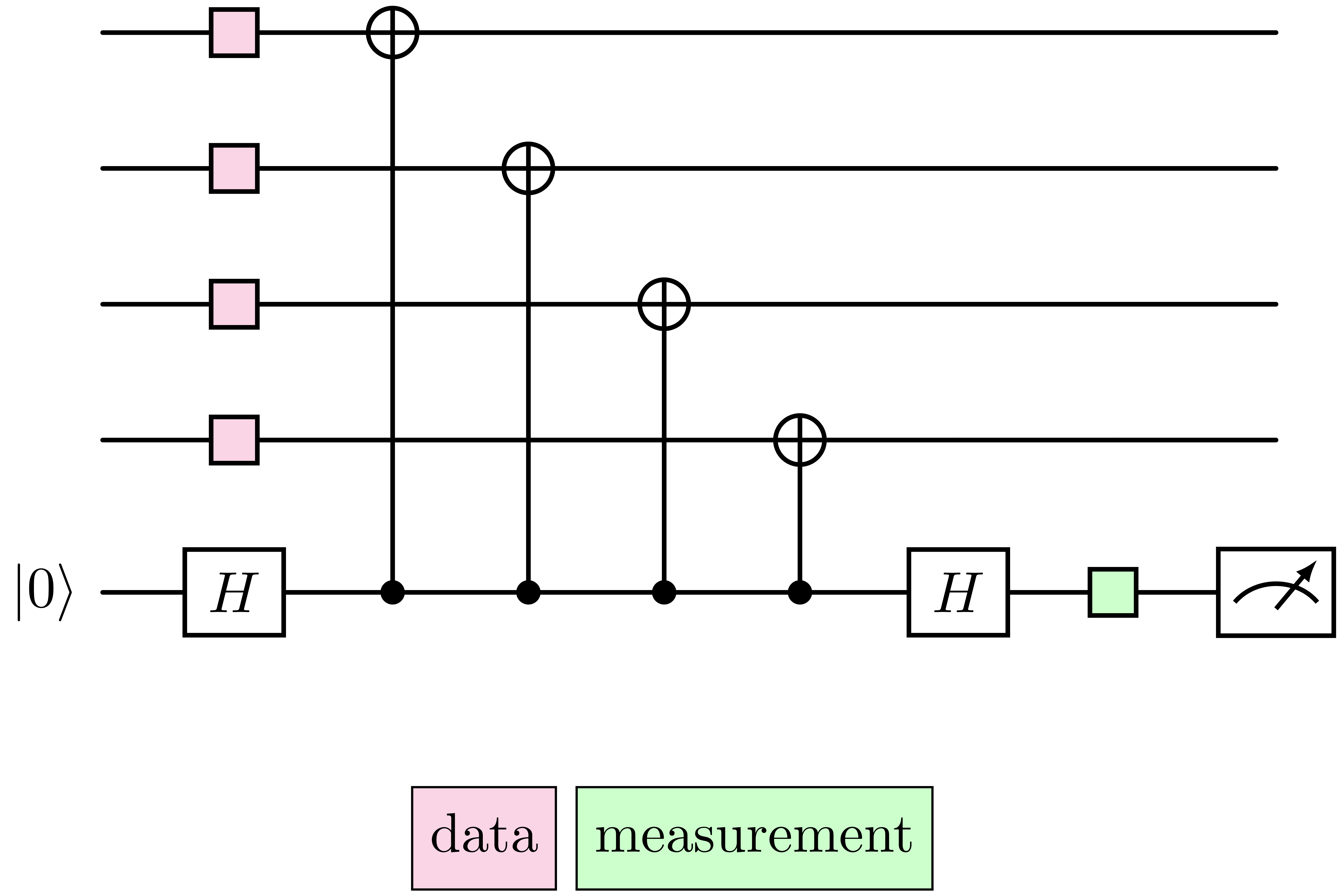
$|0\rangle$
H
H
data
measurement

$$H = \sum_{\mathbf{n}} \left[H_X(\mathbf{n} + H_Z(\mathbf{n}) + H_Y(\mathbf{n}) \right]$$

$$H_X(\mathbf{n}) = -J_x(\mathbf{n}; X)\sigma_y(\mathbf{n})\sigma_t(\mathbf{n}+\hat{y})\sigma_y(\mathbf{n}+\hat{t})\sigma_t(\mathbf{n})$$

$$-J_y(\mathbf{n}; Y)\sigma_t(\mathbf{n})\sigma_x(\mathbf{n}+\hat{t})\sigma_t(\mathbf{n}+\hat{x})\sigma_x(\mathbf{n})$$

$$-J_t^{\sigma}(\mathbf{n}; q)\sigma_x(\mathbf{n})\sigma_y(\mathbf{n}+\hat{x})\sigma_x(\mathbf{n}+\hat{y})\sigma_y(\mathbf{n})$$

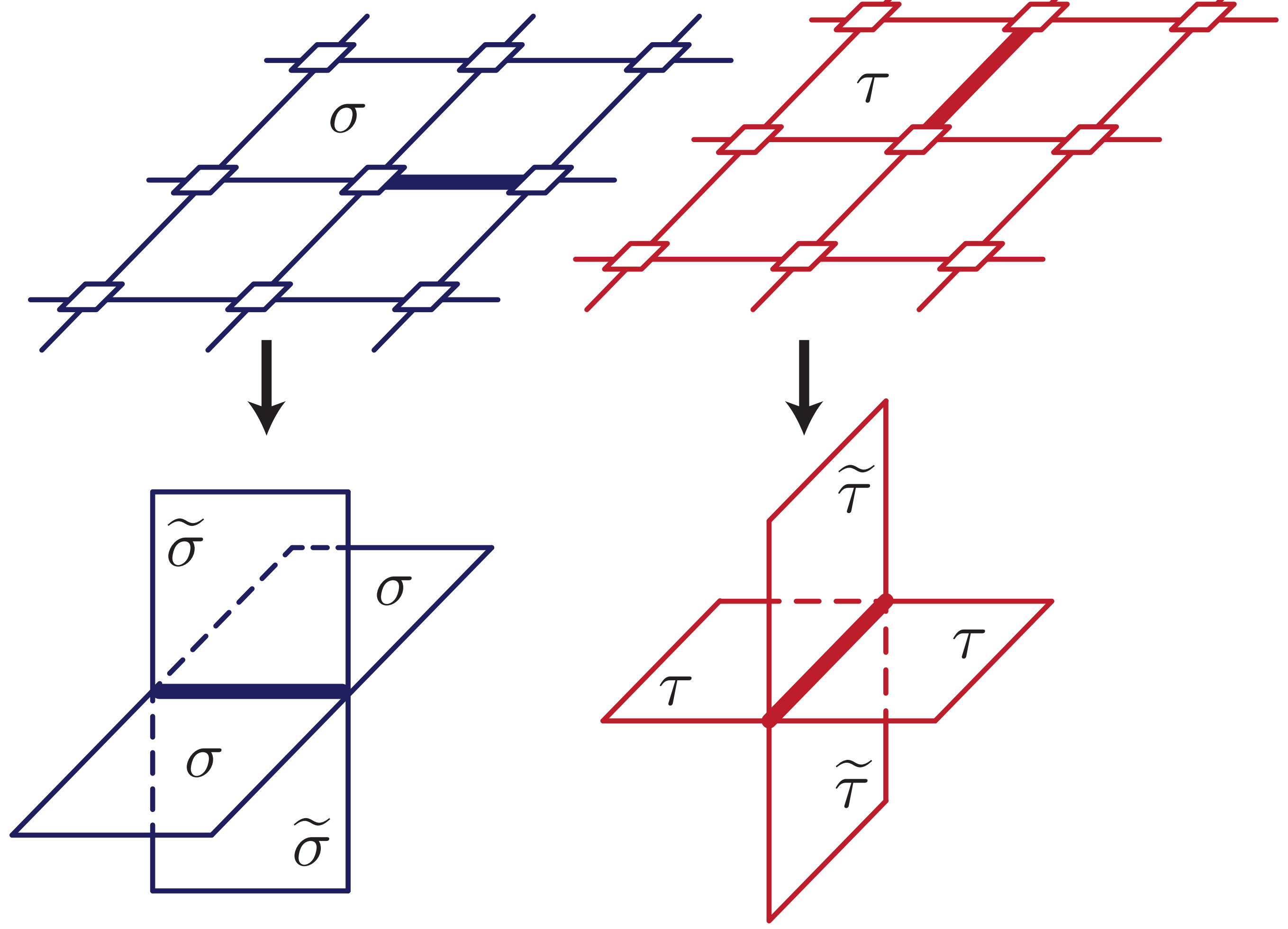

$$H_Z(\mathbf{n}) = -J_x(\mathbf{n}; X)\tau_y(\mathbf{n})\tau_t(\mathbf{n}+\hat{y})\tau_y(\mathbf{n}+\hat{t})\tau_t(\mathbf{n})$$

$$-J_y(\mathbf{n}; Y)\tau_t(\mathbf{n})\tau_x(\mathbf{n}+\hat{t})\tau_t(\mathbf{n}+\hat{x})\tau_x(\mathbf{n})$$

$$-J_t^{\tau}(\mathbf{n}; q)\tau_x(\mathbf{n})\tau_y(\mathbf{n}+\hat{x})\tau_x(\mathbf{n}+\hat{y})\tau_y(\mathbf{n})$$

$$H_Y(\mathbf{n}) = -J_x(\mathbf{n};Y)\sigma_y(\mathbf{n})\sigma_t(\mathbf{n}+\hat{y})\sigma_y(\mathbf{n}+\hat{t})\sigma_t(\mathbf{n})\tau_t(\mathbf{n}+\hat{x})\tau_x(\mathbf{n}+\hat{x}+\hat{t})\tau_t(\mathbf{n}+\hat{x}+\hat{x})\tau_x(\mathbf{n}+\hat{x})$$

$$-J_y(\mathbf{n};Y)\sigma_t(\mathbf{n})\sigma_x(\mathbf{n}+\hat{t})\sigma_t(\mathbf{n}+\hat{x})\sigma_x(\mathbf{n})\tau_y(\mathbf{n}+\hat{y})\tau_t(\mathbf{n}+\hat{y}+\hat{y})\tau_y(\mathbf{n}+\hat{y}+\hat{t})\tau_t(\mathbf{n}+\hat{y})$$

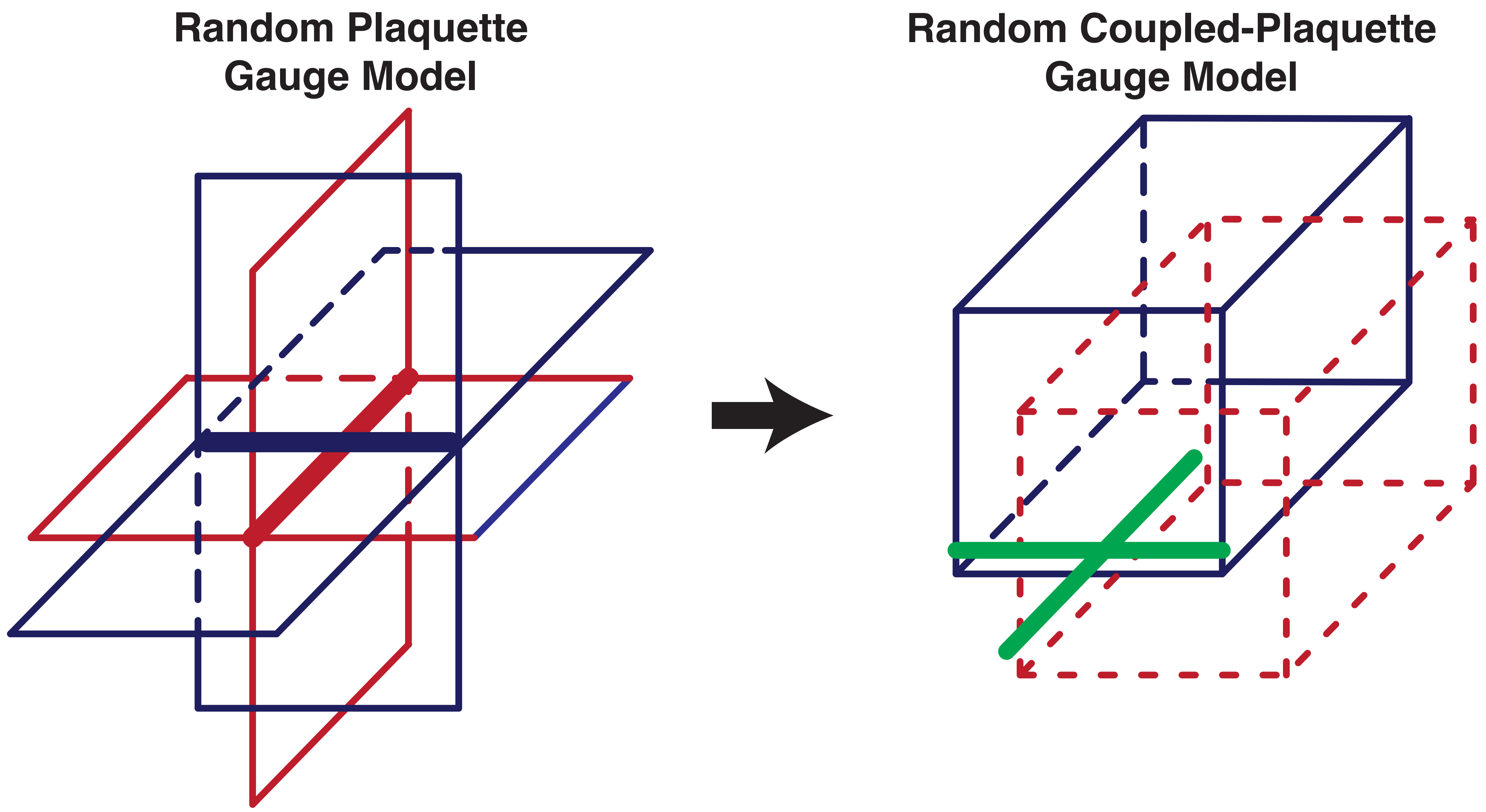

Monte Carlo Algorithm

- Metropolis algorithm for the spin–update
- Parallel Tempering for the neighboring temperature spin configuration exchange

Order Parameter:
Polyakov line

$$\langle |\overline{P}| \rangle, \;\; \overline{P} = \frac{1}{L^2} \sum_{\mathbf{x}} P(\mathbf{x}) = \frac{1}{L^2} \sum_{\mathbf{x}} \prod_{t} \sigma_{\mathbf{x},t}$$

With

$$\tilde{P} = |\overline{P}| - \langle |\overline{P}| \rangle$$

Susceptibility and the third order cumulant

$$\chi = \langle |\tilde{P}^2| \rangle, \;\; B_3 = \langle \tilde{P}^3 \rangle / \langle \tilde{P}^2 \rangle^{3/2}$$

Nishimori condition

- $\exp(-4|J(W)|) = \dfrac{\mathrm{pr}(X)\mathrm{pr}(Y)\mathrm{pr}(Z)}{(\mathrm{pr}(W))^2 p(\mathbf{1})}$
- $\exp(-2|J_q|) = \dfrac{q}{1-q}$

4. Result and Discussion

Polyakov Line, $Z(2) \times Z(2)$ gauge theory

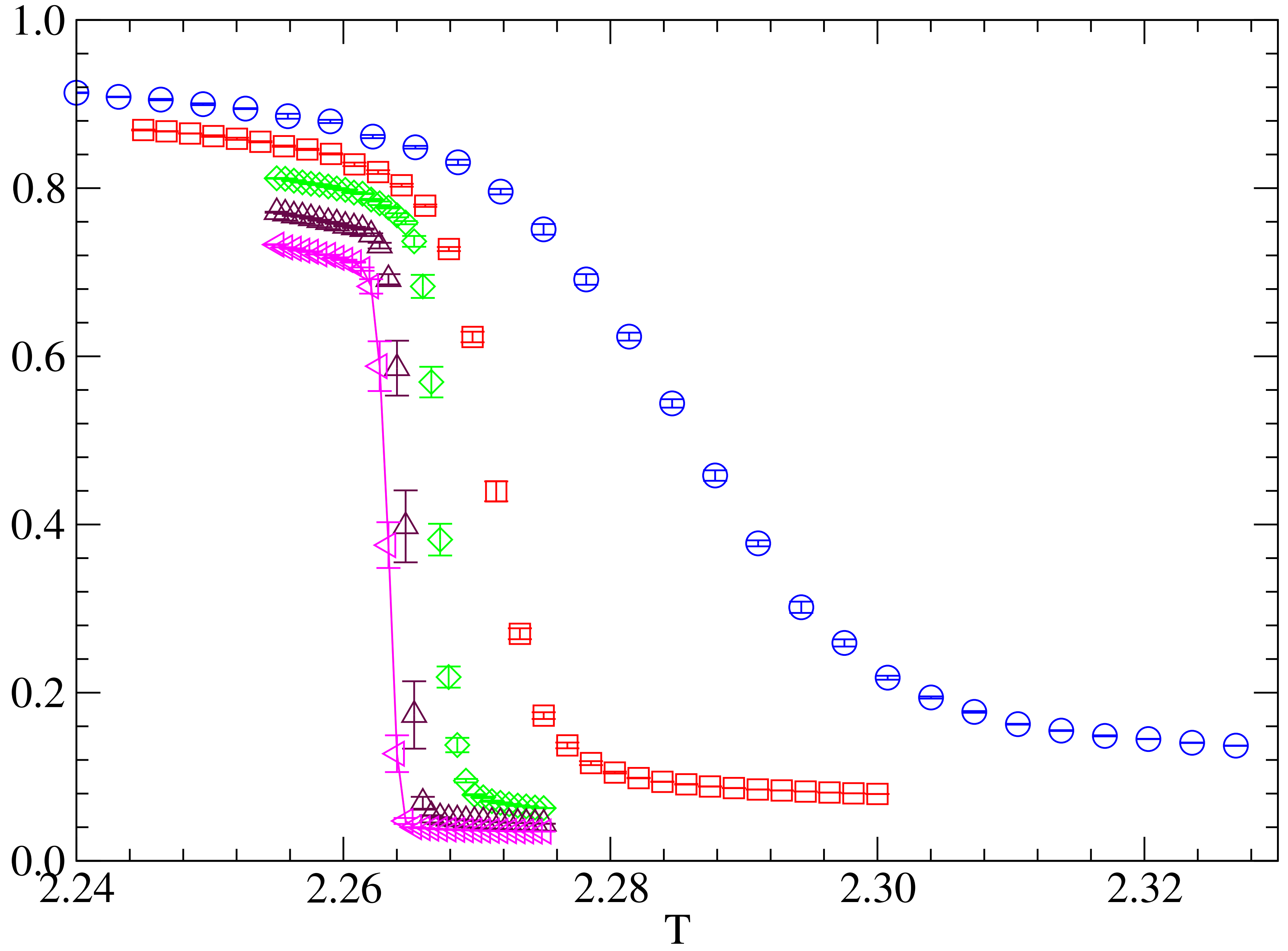

P = 2.88 x 10-5

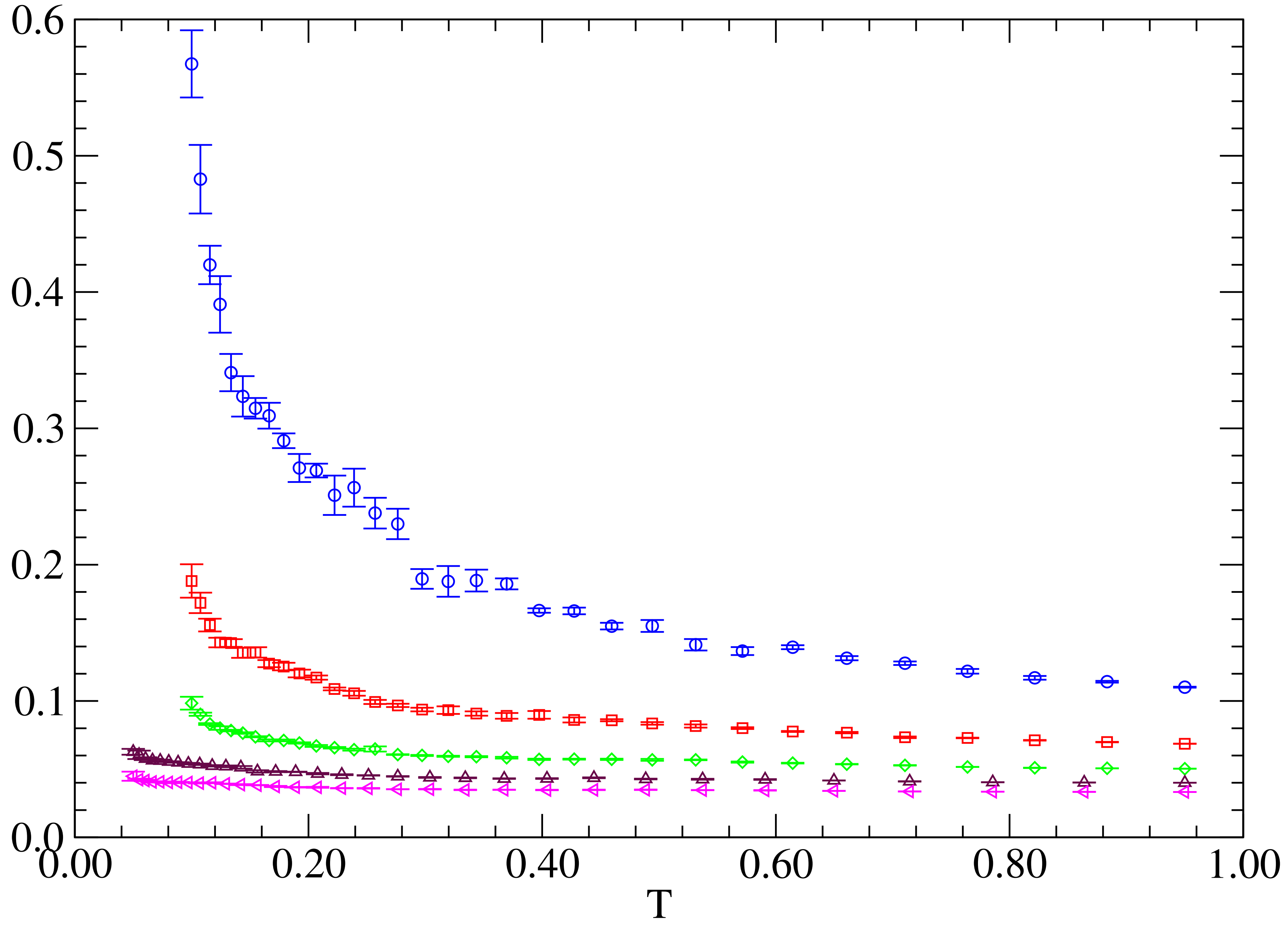

P = 0.0231

Third order cumulant of Polyakov Line, $Z(2) \times Z(2)$ gauge theory

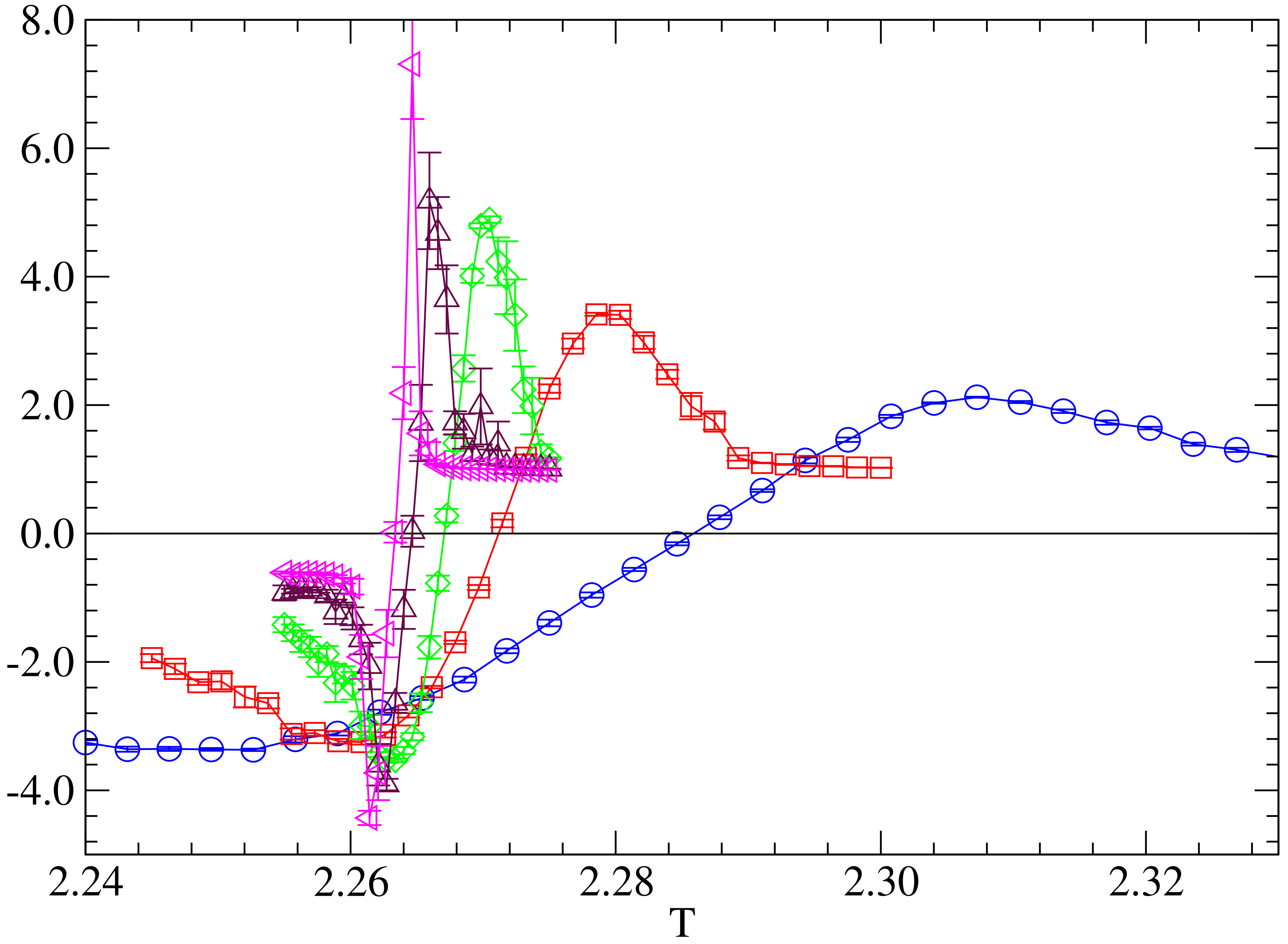

P = 2.88 x 10-5

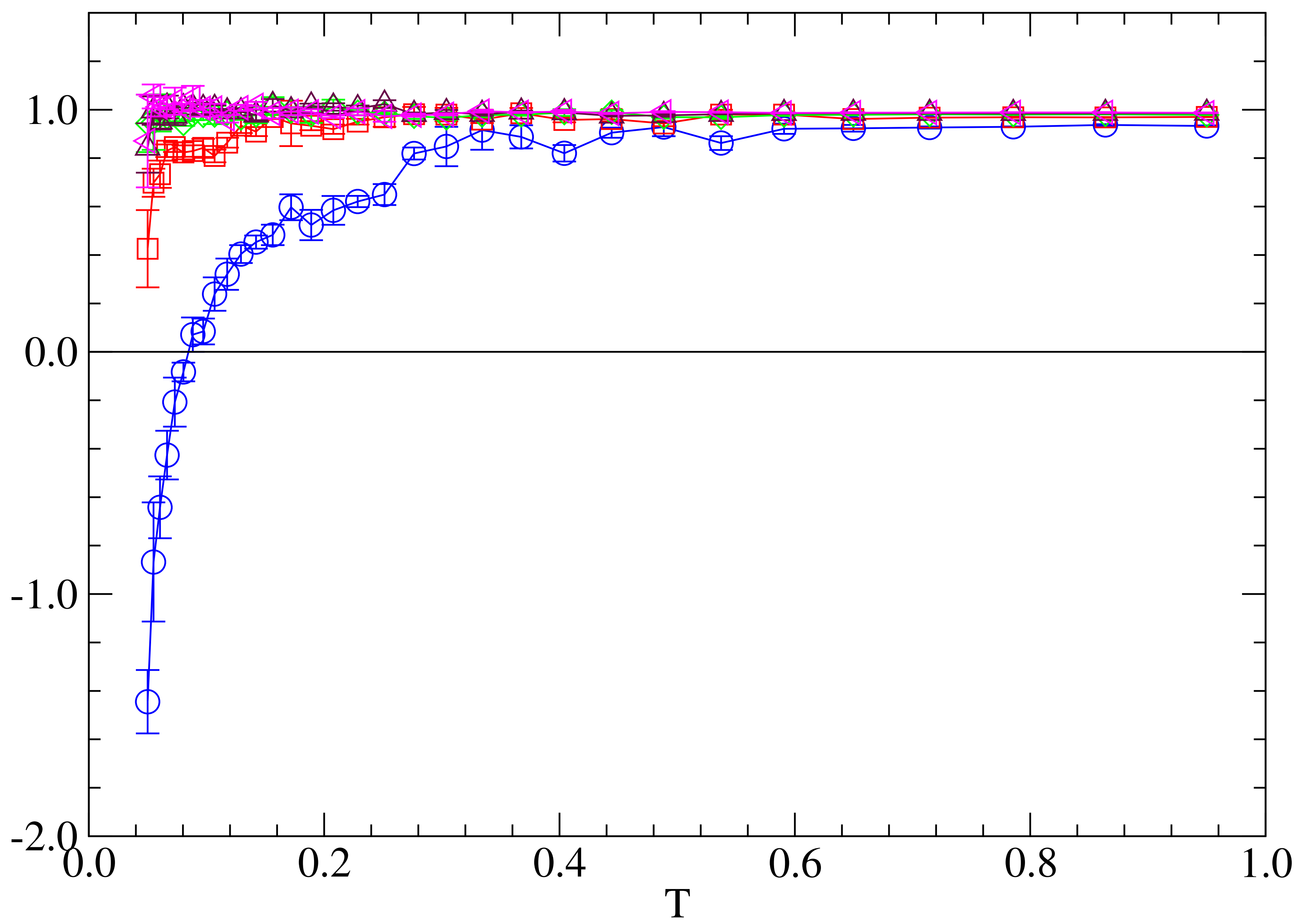

P = 0.0231

Susceptibility of Polyakov Line, $Z(2) \times Z(2)$ gauge theory

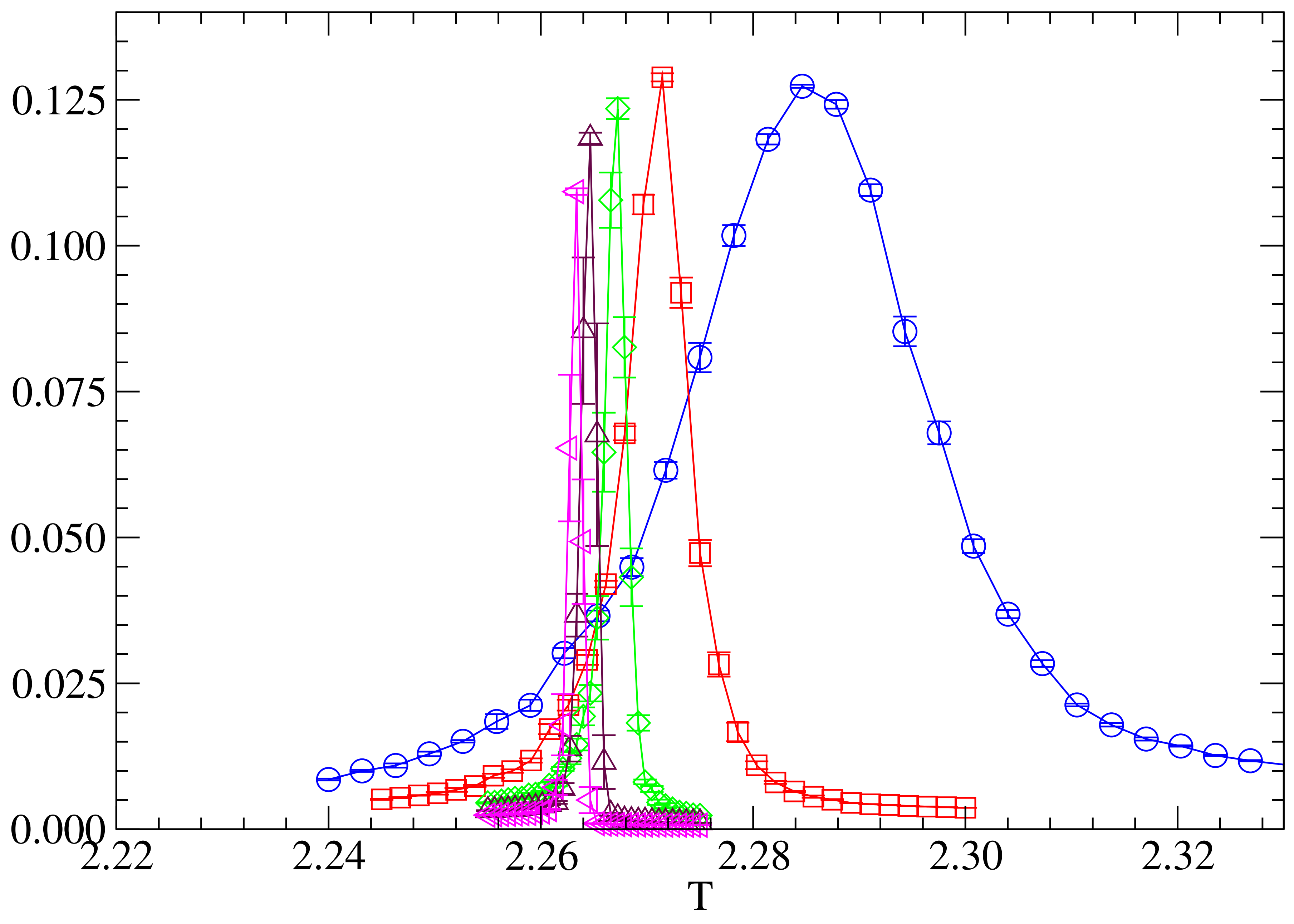

P = 2.88 x 10-5

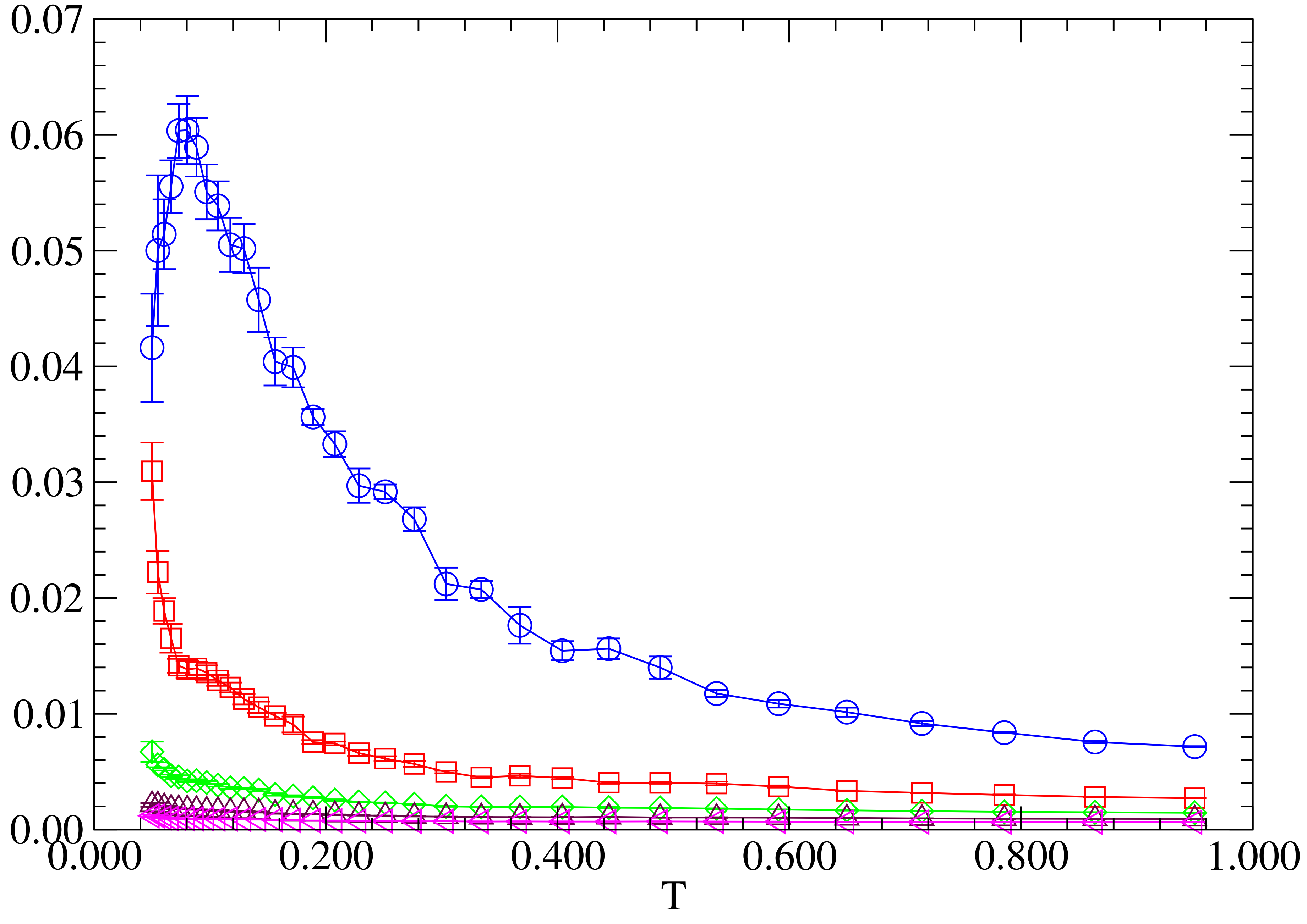

P = 0.0231

Phase diagram, $Z(2) \times Z(2)$ gauge theory

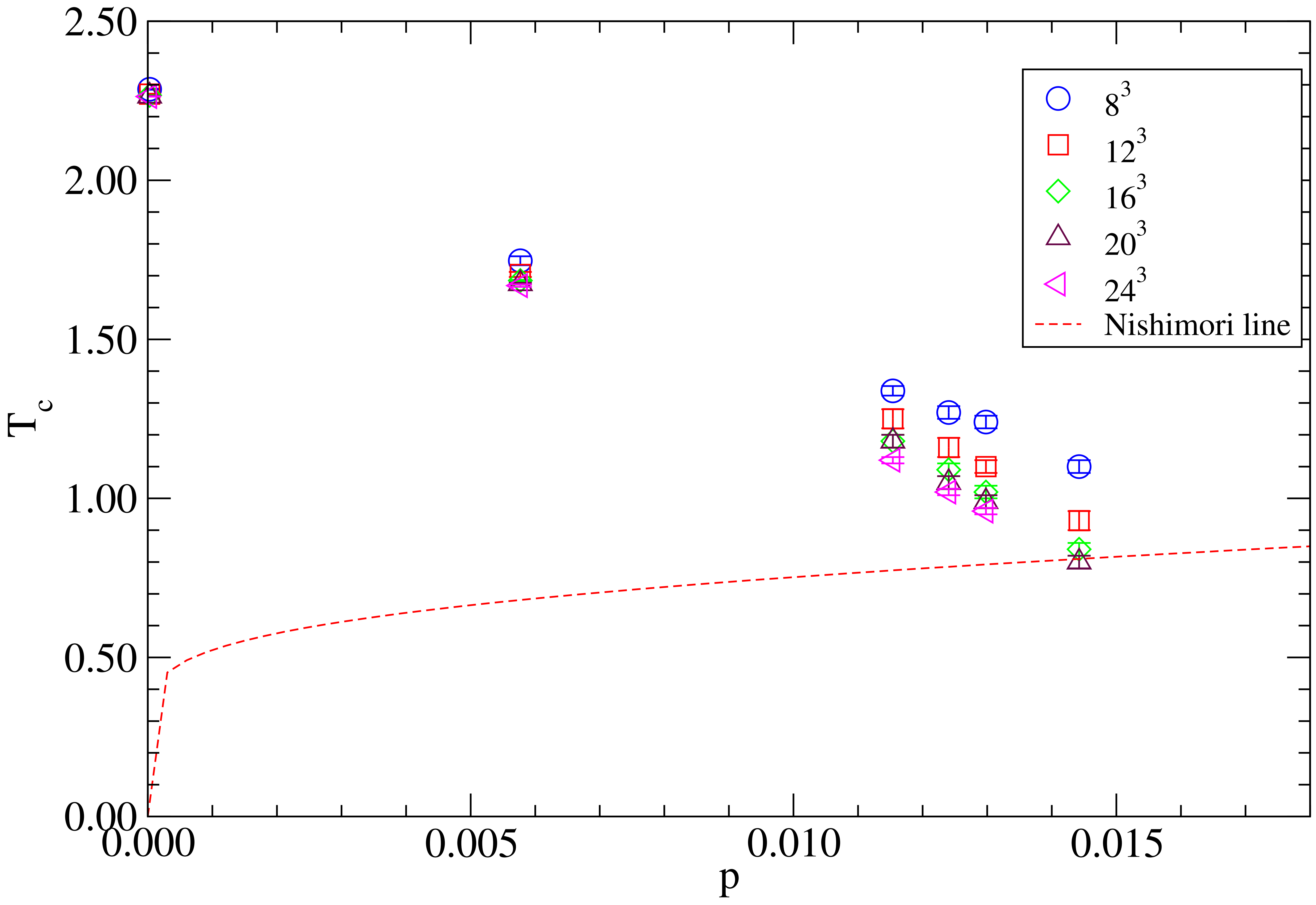

- Threshold error probability for the viability of Quantum Error Correction can be studied by MC simulation of quenched statistical physics model
- For toric code where an independent bit−flip or phase flip occurs together with independent syndrome measurement error, the threshold probability from MC suggests $p \sim 0.00682$
- For toric code where depolarizing noise occurs together with independent syndrome measurement error, the threshold probability from MC suggests $p \sim 0.0144$